

Recent advances in mechanically strong and tough hyaluronic acid hydrogels and cryogels

Oguz Okay

To cite this article: Oguz Okay (13 Oct 2025): Recent advances in mechanically strong and tough hyaluronic acid hydrogels and cryogels, Journal of Macromolecular Science, Part A, DOI: [10.1080/10601325.2025.2573075](https://doi.org/10.1080/10601325.2025.2573075)

To link to this article: <https://doi.org/10.1080/10601325.2025.2573075>



Published online: 13 Oct 2025.



Submit your article to this journal [↗](#)



Article views: 6



View related articles [↗](#)



View Crossmark data [↗](#)

Recent advances in mechanically strong and tough hyaluronic acid hydrogels and cryogels

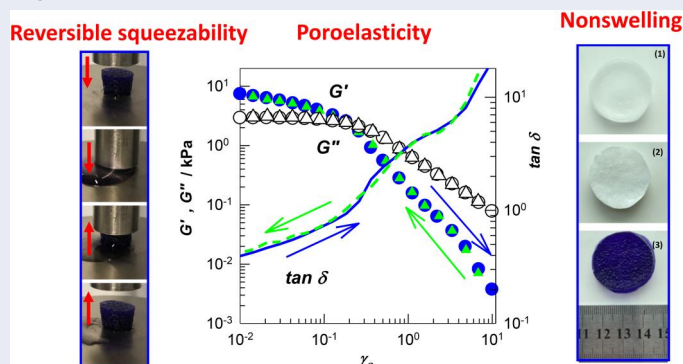
Oguz Okay

Department of Chemistry, Istanbul Technical University, Istanbul, Turkey

ABSTRACT

Hyaluronic acid (HA) is a vital extracellular matrix component renowned for its exceptional hydration, lubrication, and biocompatibility. Despite widespread use, HA hydrogels suffer from poor mechanical strength and rapid degradation, restricting their load-bearing applications. This work reviews conventional cross-linking strategies targeting HA's functional groups and highlights recent advances, particularly double-network (DN) and cryogelation methods that yield robust and resilient hydrogels and cryogels based on HA for advanced biomedical use. HA hydrogels with DN structures exhibit a fracture stress up to 12.2 MPa and a fracture strain of 94%, while the development of triple-network HA hydrogels enables resistance to compressive loads of 10–22 MPa at 95% strain, with Young's modulus values reaching up to 1 MPa, the highest mechanical performance reported for HA hydrogels to date. Furthermore, macroporous HA cryogels exhibit unique properties such as tunable poroelasticity, reversible squeezability, nonswelling behavior, and high compressive strength (up to 2.6 ± 0.2 MPa), allowing control over network mesh size and enabling precision delivery of macromolecules. Collectively, these developments represent a significant leap in HA hydrogel research, opening new avenues for their use in load-bearing tissue engineering, controlled drug delivery, and regenerative medicine.

GRAPHICAL ABSTRACT



ARTICLE HISTORY

Received August 2025
Accepted October 2025

KEYWORDS

Hyaluronic acid; hydrogels; cryogels; double networks; mechanical properties

1. Introduction

Hyaluronic acid (HA) is a naturally occurring macromolecule abundantly present in the extracellular matrix (ECM) of various tissues, such as skin, cartilage, and synovial fluid.^[1] The earliest known reference to HA dates back to 1880, when French scientist Portes observed that the mucin in the vitreous humor of the eye differed from similar substances found in the cornea and cartilage.^[2,3] He termed this substance “hyalomucin.” Decades later, in 1934, Meyer and Palmer successfully isolated HA from bovine vitreous bodies.^[4] Their analysis revealed the presence of an amino sugar and a uronic acid, inspiring the name “hyaluronic acid,” derived from “hyaloid” (meaning glass-like, in reference to the eye) and “uronic acid”. Currently, HA is

extensively utilized in biomedical and pharmaceutical fields due to its numerous distinctive characteristics, including inflammation regulation, hygroscopicity, and lubrication. It is produced by several cells, such as chondrocytes, fibroblasts, and epithelial cells, and is industrially generated *via* *Streptococcus* fermentation.^[5,6] The pronounced hydrophilicity of HA enables it to absorb and retain substantial quantities of water, rendering it an exceptional lubricant and shock absorber in joints, as well as a crucial component of ECM in connective tissues.^[7–11] Its immunosuppressive and anti-angiogenic characteristics have been investigated for the treatment of several disorders.

HA exhibits certain limitations regarding its mechanical properties and *in vivo* degradation behavior, prompting the creation of HA hydrogels with enhanced characteristics,

including improved degradation rates and biocompatibility, rendering them appropriate for applications in surgical interventions, drug delivery systems, and tissue engineering scaffolds. However, these hydrogels have weak mechanical properties, making them unsuitable for applications that involve bearing stress. This weakness is mainly because the chemically cross-linked HA network lacks effective energy dissipation, causing the hydrogels to break under even small forces.^[12,13] This review initially discusses traditional methods for synthesizing HA hydrogels utilizing the carboxyl, hydroxyl, and NHCOCH_3 groups of HA molecules. Subsequently, we discuss novel procedures for the preparation of mechanically robust and resilient HA hydrogels, mostly developed in our laboratory. The primary emphasis is on the double-network method described by Gong et al.,^[14,15] and the cryogelation technology established by Lozinsky et al.^[16,17]

2. Cross-linking of HA to make hydrogels

A prevalent technique for synthesizing HA hydrogels is cross-linking, wherein HA chains are interconnected to create a hydrogel. In comparison to natural HA, HA hydrogels exhibit enhanced chemical stability, along with superior viscoelastic properties. HA hydrogels can be rendered biocompatible by the use of appropriate cross-linkers and can be engineered to be resorbable, injectable, and antibacterial, rendering them suitable for diverse applications in the medical and cosmetic domains. HA hydrogels serve as vehicles for medication delivery, scaffolds for tissue engineering, or fillers in esthetic medicine. In tissue engineering, HA hydrogels offer a three-dimensional architecture that emulates the ECM, facilitating proliferation, differentiation, and cell adhesion. In drug delivery, HA hydrogels can protect and regulate the release of medicinal agents. In cosmetic medicine, HA hydrogels serve as dermal fillers to enhance skin appearance and diminish wrinkles.

The production of hydrogels through the cross-linking of HA can be accomplished *via* various ways, including chemical, physical, and enzymatic cross-linking.^[1,18–22] Chemical cross-linking uses chemical agents to establish covalent bonds between native or modified HA chains, whereas physical cross-linking is based on non-covalent interactions, including hydrogen bonds, hydrophobic interactions, or electrostatic forces to create a hydrogel network. In enzymatic cross-linking, enzymes such as transglutaminase are used to create covalent bonds between HA chains.^[23,24] Diels-Alder, thiol-ene, and Schiff base processes have been employed to synthesize HA hydrogels for diverse biomedical applications, including drug administration, biomolecular immobilization, scaffolding for regenerative engineering, tissue mimicry, 3D bioprinting of bioinks, and cell encapsulation.^[1,21,25–29] The characteristics of HA hydrogels may differ based on the employed cross-linking technique, necessitating a thorough evaluation of their long-term stability and biocompatibility.

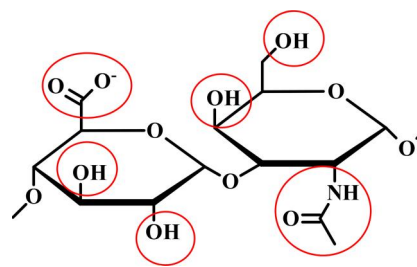


Figure 1. HA repeat units. The red circles show the functional groups for cross-linking of HA chains.

2.1. Chemical cross-linking of HA

The chemical cross-linking of HA can be achieved either by reacting native HA with suitable cross-linking agents or by using HA that has been functionalized to introduce specific reactive groups. The carboxyl, hydroxyl, and NHCOCH_3 groups present on the HA backbone are commonly exploited for such cross-linking reactions (Figure 1). Among these, hydroxyl groups are frequently targeted, enabling the formation of ether, ester, and hemiacetal linkages (Figure 2). Bisepoxides, including 1,2,3,4-diepoxybutane (DEB), ethylene glycol diglycidyl ether (EGDE), 1,4-butanediol diglycidyl ether (BDDE), and polyethylene glycol diglycidyl ether (PEGDE), are widely used to form ether bonds with HA hydroxyls.^[30] In particular, BDDE is favored due to its stability, biocompatibility, and strong ability to establish covalent HA–HA connections.^[31] Another notable cross-linker, divinylsulfone (DVS), reacts selectively with hydroxyl groups to form ether linkages, producing HA hydrogels with excellent stability, and outstanding biocompatibility (Figure 2).^[32,33] DVS cross-linking also enhances the resistance of HA hydrogels to enzymatic degradation, which is crucial for the hydrogel's longevity *in vivo*. Glutaraldehyde (GTA) serves as a cross-linker for HA, however, it necessitates an acidic environment and presents drawbacks, including instability and toxicity.^[34]

Several reagents are applicable for cross-linking through the carboxyl groups of HA, enabling the formation of amide or ester bonds with amino or alcohol groups.^[1] Cross-linking agents frequently employed include carbodiimides such as p-phenylene biscarbodiimide (BCDI) and 1-ethyl-3-(3-dimethylaminopropyl)carbodiimide (EDC), together with activating groups like N-hydroxysuccinimide (NHS), N-hydroxysulfosuccinimide (sulfo-NHS), or N-hydroxybenzotriazole (HOBt), which enhance cross-linking with amino or alcohol groups (Figure 3).^[35] EDC cross-linking facilitates a direct reaction between HA chains by activating carboxylic acids through EDC, resulting in the formation of an active acyl isourea ester. This ester subsequently reacts with neighboring hydroxyl groups, which leads to the formation of intermolecular cross-links. The cross-linking of HA with sodium alginate, a polysaccharide frequently utilized for physical gel production, has been conducted using EDC and adipic acid dihydrazide (ADH). EDC serves as a carboxyl-activating agent, while ADH acts as a cross-linker that facilitates the formation of amide bonds, potentially enhancing biocompatibility and stability.^[36]

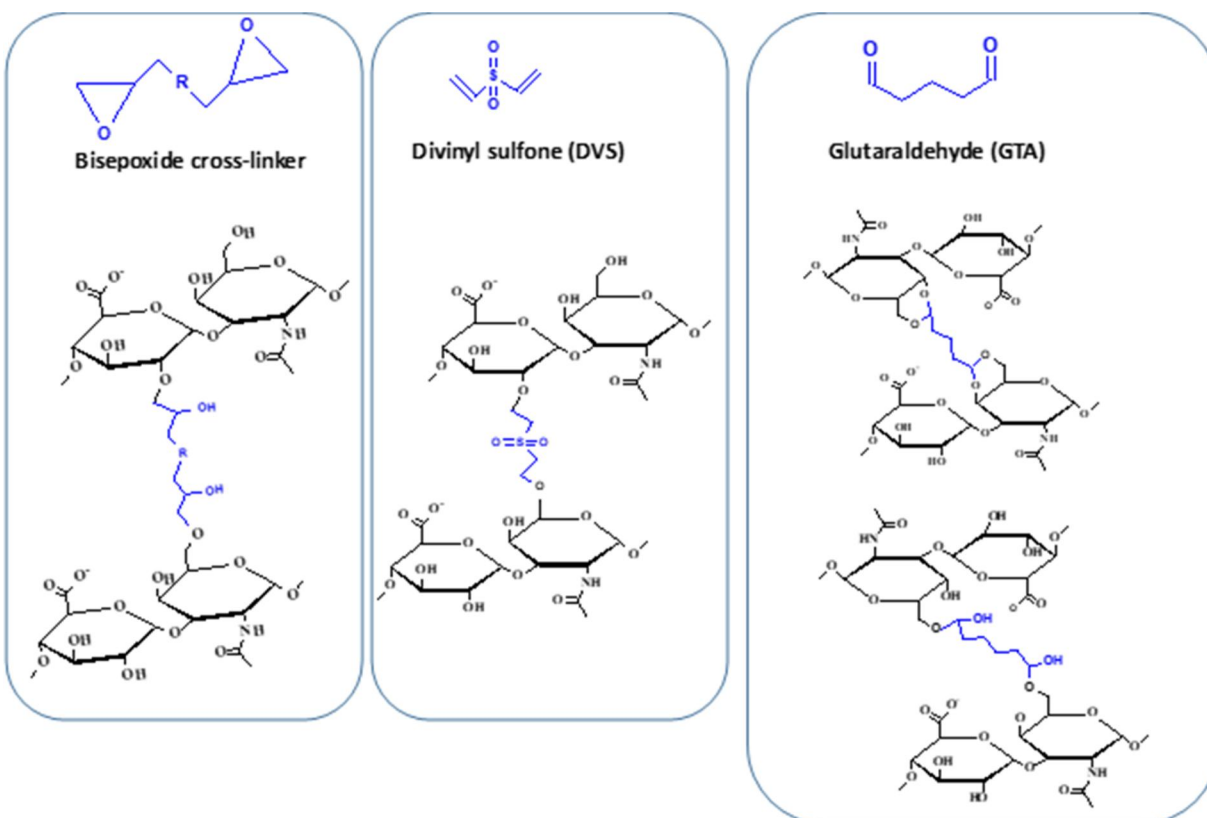


Figure 2. Upper panel: bisepoxide, divinylsulfone and glutaraldehyde for cross-linking *via* the hydroxyl groups of HA. Bottom panel: cross-linked HA units.

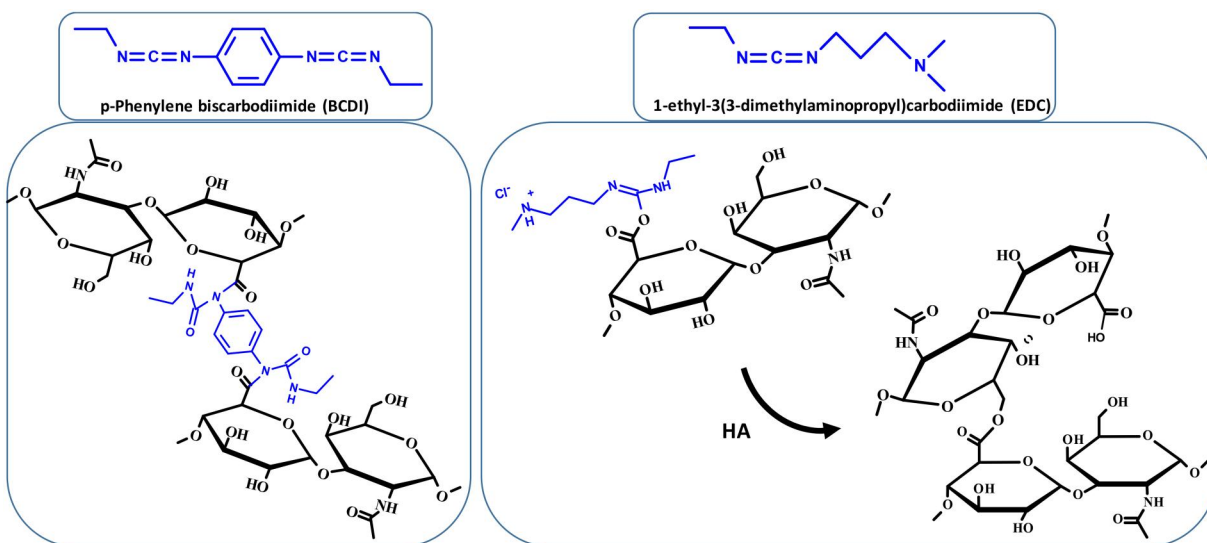


Figure 3. Chemical cross-linking of HA *via* its carboxyl groups using p-phenylene biscarbodiimide (BCDI) and 1-ethyl-3-(3-dimethylaminopropyl)carbodiimide (EDC).

The extent of cross-linking directly affects the viscoelastic properties of the resultant HA hydrogel, including elasticity, viscosity, and cohesiveness. Increased cross-linking typically results in hydrogels that are stiffer and more viscous, whereas decreased cross-linking produces hydrogels that are softer and more fluid. The selection of cross-linker and its concentration significantly influence the properties of the hydrogel. BDDE-cross-linked HA fillers exhibit greater elasticity and cohesion, whereas PEGDE-cross-linked HA fillers demonstrate increased viscosity and a higher capacity for volume expansion. Furthermore, the self-cross-linked HA

hydrogels exhibit the highest swelling rate, whereas those cross-linked with GTA demonstrate the lowest swelling rate. GTA- and DVS-cross-linked HA hydrogels exhibited robustness and elasticity when hydrated, with a glass transition temperature around 20°C. The optimal characteristics of HA hydrogels are contingent upon their intended application, such as the injection site, depth, and necessary volume of filler. The choice of a suitable crosslinker and its concentration are essential for the formulation of HA-based fillers for various applications. The molecular weight (MW) of HA, ranging from below 6×10^3 Da to above 1×10^6 Da, also

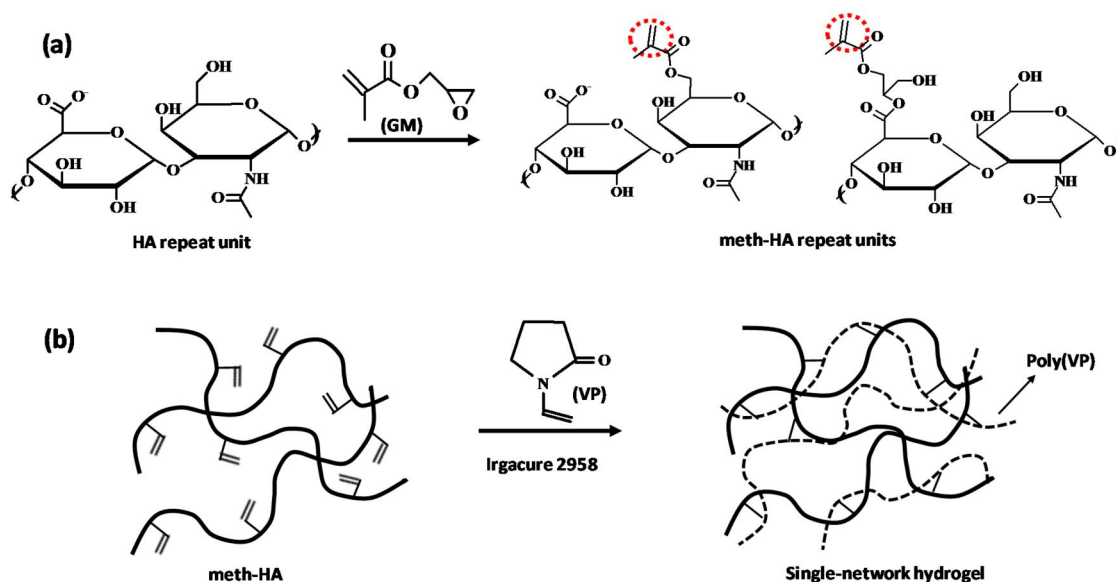


Figure 4. (a) Schemes of the preparation of meth-HA by methacrylation of native HA *via* opening of the epoxide group of GM (a), and formation of HA hydrogels (b).

governs the physical behavior of HA hydrogels, affecting gelation kinetics, mechanical stiffness, and pore structure. Hydrogels formed from higher MW HA typically gel more rapidly, display greater rigidity, and possess smaller mesh sizes, while hydrogels derived from lower MW HA polymerize more slowly, are softer, and feature larger pores.^[1,7] In addition, HA of high MW (>500 kDa) generally provides anti-inflammatory and immunosuppressive effects, whereas low MW HA (<500 kDa) can trigger pro-inflammatory responses.^[37]

Furthermore, native HA can be altered before cross-linking to produce additional functional groups, facilitating a high gel fraction, rapid cross-linking under mild reaction conditions, and improved preservation of HA chains. The oxidative cleavage of the glucuronic acid ring with periodate leads to two aldehyde groups, and the formation of Schiff bases has effectively facilitated the production of HA gel networks with adipic acid dihydrazide.^[38] A further option involves the covalent derivatization of HA chains with functionalities that can react under mild conditions with different cross-linking agents. Maleimides, phenols, amines, dienes, alkenes, and strained alkynes were covalently attached to HA, and these functionalities were cross-linked through traditional, click-chemistry, and specific enzymatic reactions.^[39] The cross-linking step facilitates the incorporation of covalently bound functional molecules, such as peptides, into the gel structure, thereby endowing the implant with enhanced functionalities, including cell adhesion *via* the RGD peptide (arginylglycylasparaginic acid).^[39] Alternatively, polymerizable functional groups, such as methacrylate groups, are attached to HA chains, enabling self-reaction under specific conditions to form a hydrogel. Photopolymerization of methacrylated HA chains, functioning as multifunctional cross-linkers, occurs under UV light in the presence of a photoinitiator, resulting in HA hydrogels with adjustable properties (Figure 4).^[40–42] Methacrylated HA (meth-HA) was synthesized through the

methacrylation of native HA (1200 kDa) in aqueous solutions utilizing varying concentrations of glycidyl methacrylate (GM).^[43] GM reacts with the hydroxyl groups on the N-acetyl-D-glucosamine units of HA *via* epoxide ring-opening, while also targeting the carboxylate groups on the glucuronic acid units through transesterification (Figure 4a). Meth-HA was subsequently photopolymerized utilizing Irgacure 2959 as the initiator and 1-vinyl-2-pyrrolidone (VP) as both the reactive comonomer and solvent, resulting in HA hydrogels with a gel fraction of unity (Figure 4b). The benefits of these reactions include (1) the ability to cross-link HA chains under milder conditions, (2) the elimination of a cross-linker that requires removal from the hydrogel, and (3) the incorporation of a novel range of functionalities on HA, which may impart new viscoelastic or biological properties to the resulting hydrogel network. The gelation process can occur *in situ*, allowing for the injection of the pre-gel solution to form a gel post-implantation.

2.2. Physical cross-linking of HA

Physical, non-covalent cross-linking is commonly employed in the synthesis of HA hydrogels; however, its primary drawback relative to covalent cross-linking is the hydrogel's long-term instability. Hydrogen bonds, hydrophobic interactions, ionic interactions, and metal ion coordination have been utilized to create physical HA hydrogels.^[1,5] Many supramolecular hydrogels made with HA and based on hydrogen bonding have been developed for biomedical use. For example, Ye et al. created an injectable hydrogel that relies entirely on hydrogen bonds to form its structure.^[44] In this system, HA chains were modified with cytosine and guanosine units, which can form complementary base pairs, allowing the chains to stick together through hydrogen bonding. When mixed in phosphate-buffered saline (PBS), the hydrogel formed in just 6 min and reached a storage modulus (G') of 100 kPa, showing adequate good mechanical

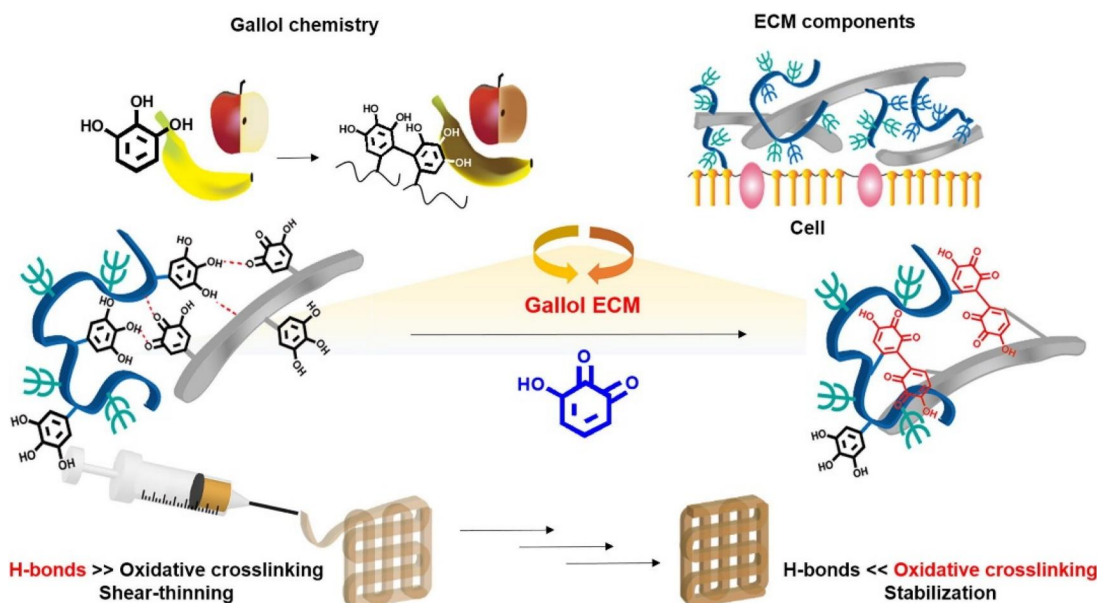


Figure 5. Schematic explanation of the formation and extrusion of gallol-derived ECM-mimetic adhesive bioinks.^[47]

strength. These hydrogels also have self-healing abilities because the physical interactions between chains are temporary and reversible. This property also allows them to be easily injected into the body.

Chen et al. developed an HA-based supramolecular nanocomposite hydrogel for delivering the anticancer drug doxorubicin.^[45] They created nanoconjugates by linking HA (with a molecular weight of 10 kDa) to silica using a base-catalyzed condensation reaction involving tetraethoxysilane and a surfactant called cetyltrimethylammonium bromide. The resulting particles were mesoporous silica nanoconjugates, coated with HA. These had pores about 2 nm wide and an overall particle size of 200–300 nm. When placed in a solution at pH 6.8, the HA coating helped the nanoconjugates form a hydrogel. The particles began to stick together through hydrogen bonding between HA chains, causing them to grow into larger clusters, up to 10,000 nm in size, and form a 3D network structure.

Hydrogen-bonded HA hydrogels have also been studied for uses beyond drug delivery, especially as wound dressings. Zhang et al. developed a nanocomposite hydrogel made from polyvinyl alcohol (PVA), silver (Ag) nanoparticles, and high-molecular-weight HA (1200 kDa) for its biocompatibility and ability to absorb fluids.^[46] The hydrogels were made using a freeze-thaw process, which creates small crystalline areas in the PVA that act as physical cross-links. Silver nanoparticles (20–50 nm) were added by exposing silver nitrate (AgNO_3) in the hydrogel to UV light, causing silver to form within the HA/PVA matrix. The resulting HA/PVA/Ag hydrogels showed much better antibacterial activity than hydrogels made from only HA/PVA or just PVA. Because of these strong antibacterial effects and advantageous swelling properties, these hydrogels are promising materials for wound care.

Supramolecular hydrogels that use hydrogen bonding and contain HA have also been studied for 3D printing in tissue engineering. One example is a hydrogel ink made from

gallol-modified HA and gelatin, which forms a network through hydrogen bonding between gallol groups (Figure 5).^[47] In this system, HA (151–300 kDa) and gelatin were chemically modified using 5-hydroxydopamine through EDC/NHS coupling, resulting in a gallol content of about 10–15%. When these modified polymers are mixed, they self-assemble quickly to form a hydrogel under physiological conditions. The hydrogel structure is stabilized by hydrogen bonds between gallol units, as well as between gallol and the gelatin protein. This makes the material suitable for 3D bioprinting applications in tissue engineering. The supramolecular hydrogel demonstrates shear-thinning behavior immediately post-gelation, attributable to reversible hydrogen bonds, thus rendering it appropriate for 3D extrusion printing. 3D printing utilizing encapsulated fibroblasts demonstrated successful execution, yielding a high cell viability of 95%. The HA- and gelatin-based bio-ink presents a promising method for fabricating constructs in soft tissue engineering applications, attributed to its rapid and efficient hydrogen bond self-assembly followed by covalent cross-linking and stabilization.

Physical HA hydrogels were also generated through hydrophobic interactions by incorporating thermo-responsive polymers, specifically poly(*N*-isopropylacrylamide) (PNIPAM), into the hydrogel network. PNIPAM is a commonly used temperature-responsive polymer that undergoes a reversible sol-gel transition around 32 °C, which is close to body temperature.^[48,49] HA is commonly conjugated with PNIPAM to create amphiphilic polymers. In this arrangement, HA contributes hydrophilicity and swelling characteristics to the hydrogels, while the thermo-responsive nature of PNIPAM facilitates self-assembly. Chou et al. prepared supramolecular hydrogels composed of PNIPAM, chitosan, and HA (1800 kDa) to prevent postoperative peritendinous adhesions in tendon surgery.^[50] HA-PNIPAM-based hydrogels have been documented in multiple studies for applications in cell

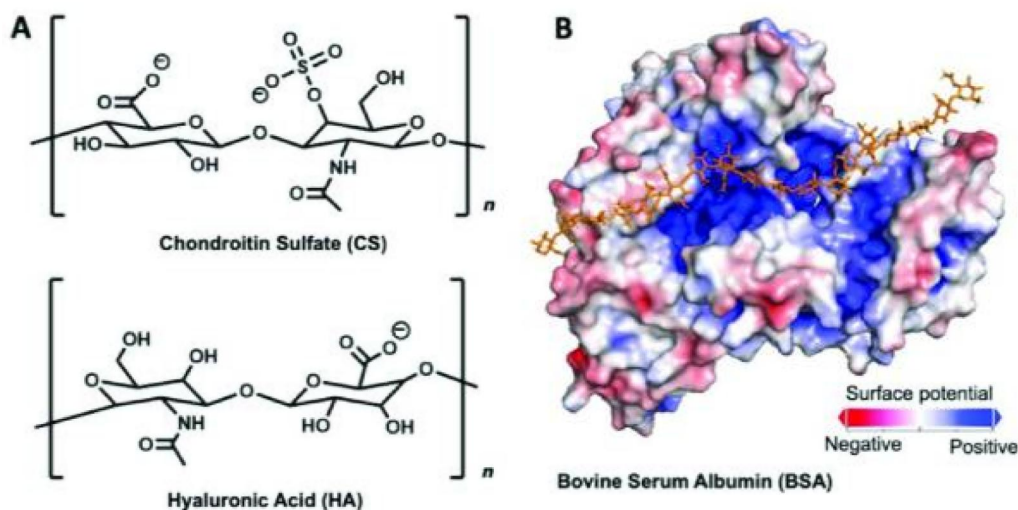


Figure 6. (A) Chemical structures of chondroitin sulfate (CS) and HA. (B) Schematic illustration of the relative surface charge densities of bovine serum albumin (BSA). The HA chain is shown interacting with the positively charged binding pocket of BSA.^[51]

encapsulation, drug delivery, tissue engineering, and as reservoirs for antibiotics.^[5]

Ionic (electrostatic) interactions are useful in forming supramolecular HA hydrogels because of their rapid kinetics and good response to changes in the environment. At physiological pH, HA carries negatively charged carboxyl groups, allowing it to easily form complexes with positively charged molecules. This phenomenon makes it relatively easy to create HA-based hydrogels using ionic interactions. Tabet et al. studied this approach by combining HA with chondroitin sulfate (CS) and bovine serum albumin (BSA) to mimic the environment of central nervous system tissue (Figure 6).^[51] Although BSA is generally negatively charged at physiological pH, it contains positively charged regions (cationic binding pockets) that can interact with negatively charged glycosaminoglycans like HA and CS. In its folded state, BSA possesses a single binding site; however, upon heating, it is capable of interacting with multiple polysaccharide chains. The supramolecular HA/CS/BSA gel offers an enhanced method for investigating drug diffusion in a hydrophilic environment, as it more accurately simulates tissue compared to traditional diffusion in saline. Micelle aggregation represents an alternative method for the formation of HA hydrogels through ionic interactions, effectively ‘gluing’ polymers like HA into a hydrogel structure. Micelle-forming carboxymethylhexanyl chitosan (CHC) can form hydrogels when combined with low molecular weight HA (15–30 kDa) through electrostatic interactions between the polymer and nanoparticles.^[52]

Metal coordination bonds are a type of non-covalent interaction formed between a metal ion and a ligand, a molecule that donates an electron pair to the metal. If the ligand has two or more binding sites, it can form several bonds with the same metal ion, creating a stronger interaction called chelation. The strength of coordination bonds can vary depending on the specific metal and ligand. Because these bonds are reversible, they are useful in making supramolecular hydrogels. A common example is alginate, which forms hydrogels when it interacts with calcium ions (Ca^{2+}).

An example of an HA-based supramolecular hydrogel using metal coordination bonds was developed by Miyazaki et al.^[53] In this system, HA was cross-linked with the antibiotic doxycycline in the presence of a divalent metal ion. Doxycycline contains a positively charged dimethylammonium group, which can interact with the negatively charged carboxylate groups on the HA chains, helping to form the hydrogel network. The compound features a phenolic diketone functionality that facilitates chelation between two doxycycline molecules in the presence of divalent ions like Mg^{2+} , leading to cross-linking and the establishment of a physical network. This hydrogel system has the potential for doxycycline delivery, with release profiles influenced by the drug-to-HA ratio. Hydrogels made from HA and metal coordination bonds have been studied as cell carriers for neural transplantation therapies. Nakaji-Hirabayashi et al. developed such a hydrogel using HA and recombinant peptides that form coordination bonds with metal ions, allowing the hydrogel to function effectively as a cell delivery system.^[54] Research has also been conducted on supramolecular nanocomposite hydrogels composed of HA and silica nanoparticles, which are cross-linked through metal coordination bonds for the purpose of drug delivery.^[55]

3. Mechanically robust and resilient HA hydrogels

A limitation of HA hydrogels is their brittleness and susceptibility to dissolution in physiological environments, which restricts their application in load-bearing scenarios. The sub-optimal mechanical performance of covalently cross-linked HA hydrogels can be attributed to their insufficient resistance to crack propagation, resulting from the absence of an effective energy dissipation mechanism within the gel network.^[12,13] Moreover, the degradation of HA chains in aqueous solution during cross-linking reactions leads to a reduction in molecular weight, resulting in weak hydrogels.^[56] The following discussion focuses on double-networking and cryogelation techniques for the production of HA-based hydrogels exhibiting superior mechanical properties.

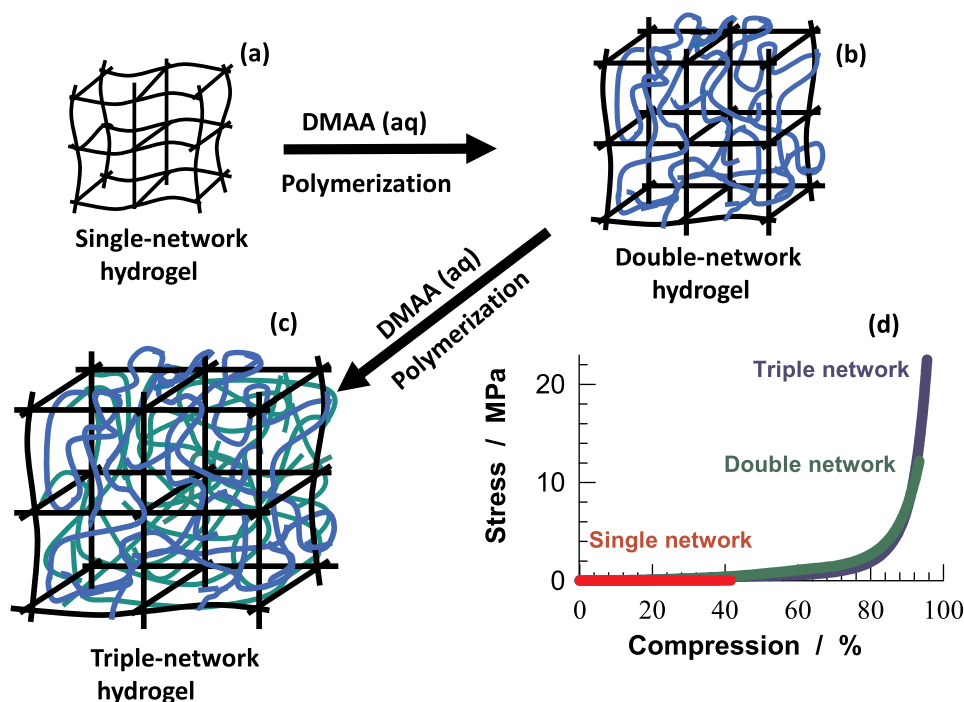


Figure 7. Schematic illustration of the formation of (a) single-network, (b) double-network, and (c) triple-network hydrogels based on HA. (d) Compressive stress–strain curves of the corresponding hydrogels: single-network (red), double-network (green), and triple-network (dark blue).^[43]

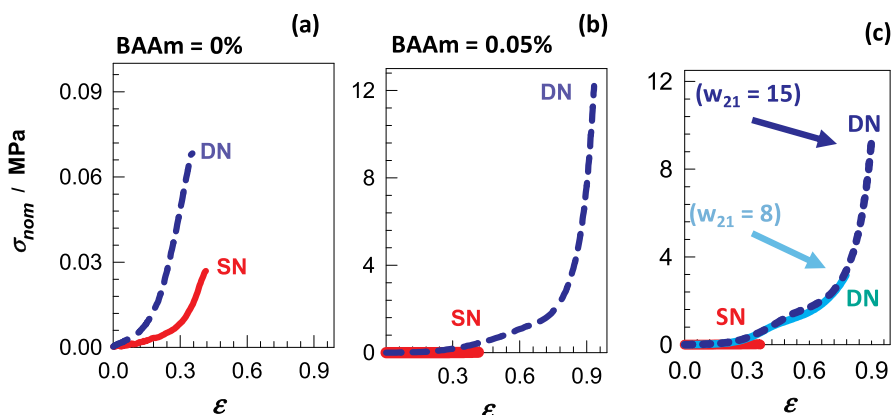


Figure 8. (a, b) Compressive stress–strain curves of HA hydrogels with single-network (SN, solid red curves) and double-network (DN, dashed blue curves) structures. The amount of BAAm used in the second network is indicated. (c) Effect of the mass ratio w_{21} (second network to first network repeat units) on the compressive stress–strain behavior of HA hydrogels with DN structure.^[43]

3.1. Double- and triple-network hydrogels based on HA

Recent advancements in hydrogels have introduced novel approaches for the production of mechanically robust hydrogels exhibiting high toughness. The double-networking technique, developed by Gong and colleagues, is one of these strategies.^[14,15,57] Double-network (DN) hydrogels are composed of two interpenetrating and interconnected networks that exhibit contrasting mechanical properties, as illustrated in Figure 7a,b. The initial single network (SN) exhibits strong cross-linking, resulting in brittleness, whereas the secondary network, which constitutes the primary component, possesses a loosely cross-linked architecture. Upon the application of force, the initial network fails at a comparatively low load by dissipating energy, whereas the ductile secondary network maintains the integrity of the hydrogel. Initially, an SN hydrogel with a high cross-linker

content is synthesized to produce a DN hydrogel. The brittle SN hydrogel is immersed in a second monomer solution that includes a small quantity of cross-linker and an initiator, leading to polymerization. This process results in DN hydrogels characterized by high mechanical strength and an exceptional breaking stress of approximately 20 MPa.

Weng et al. were the first to report HA-based double-network (DN) hydrogels that contain 60–90% water and show impressive mechanical strength, with a compressive modulus of 0.5 MPa and a breaking stress of 5.2 MPa.^[58] To make these hydrogels, they first created a stiff, highly cross-linked network using methacrylated HA (meth-HA). This network was then swollen in a solution containing the monomer N,N-dimethylacrylamide (DMAA) and a small amount of cross-linker. Afterward, DMAA was polymerized to form a second, softer, and loosely cross-linked network of poly(N,N-dimethylacrylamide) (PDMAA). The resulting

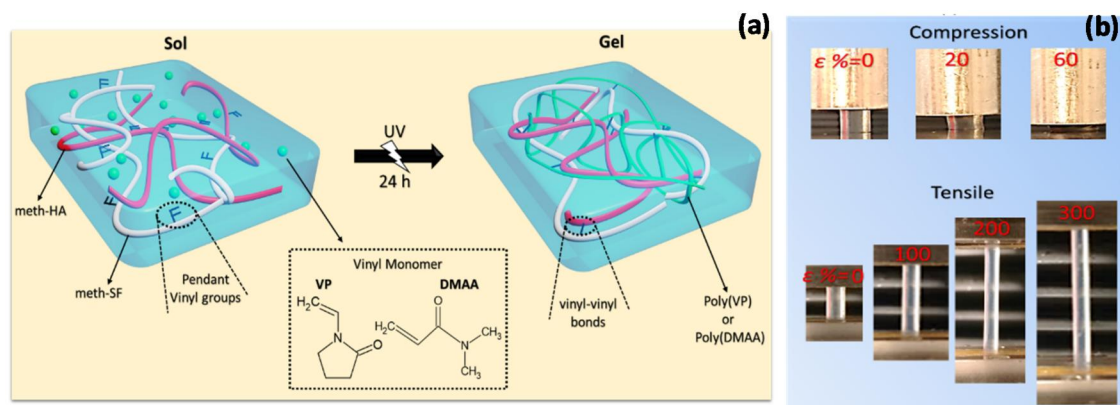


Figure 9. (a) Schematic illustration of the preparation of meth-HA/meth-SF hydrogel in the presence of DMAA and (VP). (b) Digital photographs of the meth-HA/meth-SF hydrogel under compression and tensile tests at various applied strains, as indicated.^[59]

hydrogel consists of two interpenetrating networks: a brittle meth-HA network and a ductile PDMAA network. When the material is under high stress, the stiff meth-HA network cracks, but the softer PDMAA network holds the structure together. This combination greatly improves the mechanical performance of the overall hydrogel.

The enhancement of the mechanical properties of HA hydrogels following double-networking is depicted in Figures 8a and 8b, which present the compressive stress-strain curves for meth-HA first-network (SN) and meth-HA/PDMAA double-network (DN) hydrogels.^[43] Meth-HA hydrogels prior to double-networking exhibit brittleness, rupturing at approximately 40% compression (solid red curves). The introduction of the second network in the hydrogel network results in a significant improvement in mechanical properties (dashed blue curves). The fracture stress and fracture strain of the DN hydrogel based on HA containing a small quantity of N, N'-methylene bis(acrylamide) (BAAm) cross-linker increase from 0.03 to 12.2 MPa and from 40% to 94%, respectively, following double networking (Figure 8b).^[43]

The mass ratio (w_{21}) of the second to the first network units is a critical parameter influencing the mechanical strength of HA hydrogels.^[43] Optimal mechanical performance necessitates a significant concentration of the second network relative to the first, specifically a high mass ratio between these networks. Figure 8c illustrates the dependence of the stress-strain curves of DN hydrogels based on meth-HA on the w_{21} ratio, demonstrating a significant increase in fracture stress with a higher w_{21} ratio. For example, SN hydrogels derived from meth-HA demonstrate a Young's modulus of 17 kPa, which increases to 370 kPa following double-networking at $w_{21} = 15$.^[43] The significant rise in the modulus E during the formation of double-network structures reflects a substantial level of physical and chemical connectivity among the network components of DN hydrogels. Comparable outcomes were observed when native HA was utilized in place of meth-HA in the double-networking process, achieved by forming cross-links between the HA chains through the chemical cross-linker EGDE.^[56]

A triple-network strategy has been developed to create mechanically robust HA hydrogels, as illustrated in Figure

7c.^[43] TN hydrogels were synthesized by swelling DN hydrogels in aqueous DMAA solutions containing BAAm cross-linker and 2-oxoglutaric acid as an initiator, followed by photopolymerization. TN hydrogels can endure compressive loads ranging from 10 to 22 MPa at 95% compression and demonstrate a Young's modulus E of up to 1 MPa (Figure 7d). The values presented represent the maximum fracture stresses for HA hydrogels documented in the existing literature. The development of TN hydrogels utilizing HA and PDMAA marks a notable progression in HA hydrogel research, with prospective applications in load-bearing biomedical contexts.

3.2. Tough and stretchable hydrogels based on methacrylated derivatives of HA and silk fibroin

There is a significant demand for soft materials that replicate ECM in tissue engineering applications. Recent studies have reported ECM-inspired hydrogels characterized by high compressibility and extensibility, utilizing HA and silk fibroin (SF).^[59] To enhance the mechanical properties of HA/SF hydrogels, methacrylated derivatives of HA (meth-HA) and SF (meth-SF) were employed concurrently as macromers and macrocross-linkers, resulting in a dual macrocross-linker system (Figure 9a). The hydrogels were made using vinyl monomers DMAA and 1-vinyl-2-pyrrolidone (VP), which act as spacers to create highly elastic polymer chains. These chains are connected by a dual cross-linker system made of meth-HA and meth-SF. Without the monomers, the meth-HA/meth-SF hydrogels had a low Young's modulus (below 4 kPa), meaning they were quite soft. Adding the monomers greatly improved their mechanical strength: the Young's modulus increased from 4 to 36 kPa, and the fracture stress rose from 1.4 to 4.2 MPa in compression tests and from 6 to 15 kPa in tension tests.^[59] These hydrogels can be compressed up to 60% and stretched up to 300% (Figure 9b). X-ray diffraction (XRD) analysis showed that meth-SF mainly exists in random coil or helical shapes, not forming rigid β -sheet crystals. This flexible structure improves the hydrogel's stretchability, compressibility, and resistance to fatigue. Because of their adjustable properties and extracellular matrix (ECM)-like structure,

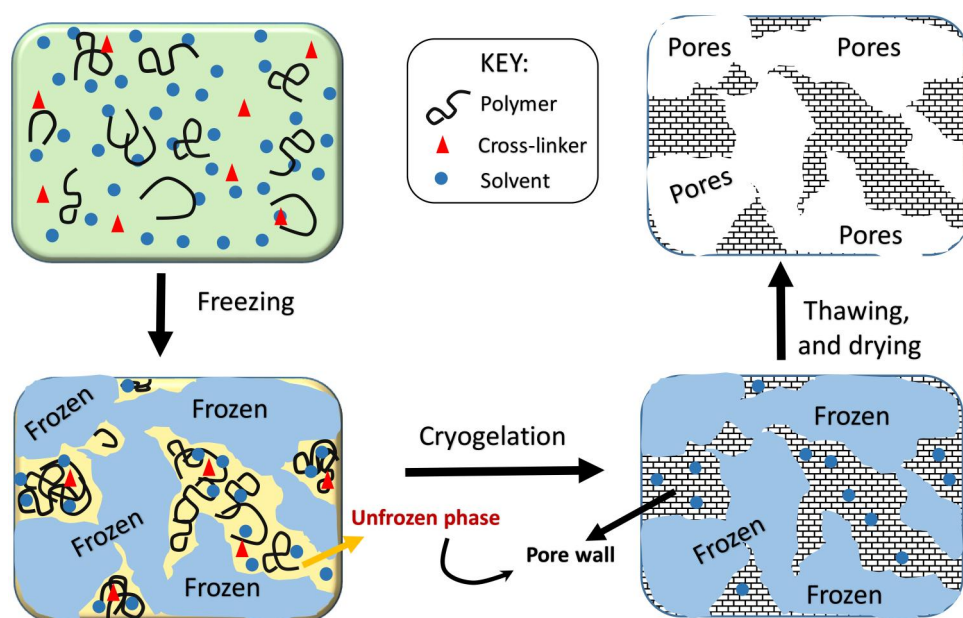


Figure 10. Cartoon illustration of cryogelation in a polymer solution containing a chemical crosslinker.^[70]

meth-HA/meth-SF hydrogels are promising materials for soft tissue engineering applications.

3.3. HA cryogels

Cryogelation is an effective method for producing macroporous and resilient hydrogels, referred to as cryogels. Despite the discovery of cryogelation reactions and cryogels over 70 years ago,^[60–62] significant interest has only emerged in the past two decades.^[16,17,62–69] This surge is primarily due to their remarkable properties relative to traditional hydrogels, including high toughness, near-complete squeezability, a mechanically stable porous structure characterized by a honeycomb arrangement, poroelasticity, and rapid responsiveness to external stimuli. The main method for making cryogels involves freezing water-based solutions of polymers or monomers, then cross-linking them. Unlike regular gelation, which happens at or above room temperature, cryogelation takes place at temperatures 10 to 20°C below the freezing point of the solution. At these cold temperatures, most of the water freezes, but a small amount stays liquid because of the high concentration of monomers or polymers in those areas (Figure 10).^[70] This process, called cryoconcentration, causes the monomers or polymers to gather in the unfrozen pockets, where they polymerize and cross-link. The ice crystals act as templates, around which thick and elastic pore walls form, creating the characteristic porous structure of cryogels.

The initial preparation of cryogels utilizing HA was accomplished a decade ago by Ström and colleagues.^[71] HA cryogels were synthesized from frozen aqueous solutions of HA utilizing EGDE as a cross-linking agent. Responsive and mechanically stable HA cryogels with high toughness and interconnected macropores were achieved by adjusting the synthesis conditions.^[71] The findings indicate that an HA cryogel forms exclusively within a specific range of subzero

temperatures, exhibiting a rapid swelling rate, although its volume does not significantly increase. Cryogels were successfully formed at HA and EGDE concentrations of 7.3% and 1.7%, respectively, when the temperature was lowered to -10°C and -18°C . However, no gelation occurred at 0°C because the solution did not freeze. Gelation happens only below the freezing point because HA and EGDE become highly concentrated in the small unfrozen areas of the frozen solution.^[16,17] This cryoconcentration means the local concentrations of HA and EGDE in these regions are much higher than their average amounts in the whole solution. Although low temperatures slow down the cross-linking reaction, this is balanced out by the high local concentrations of HA and EGDE, allowing gelation to proceed. Gelation did not occur at 0°C due to the equality of the actual and nominal concentrations of the reactants.

HA cryogels exhibit significant resilience, allowing for compression of approximately 80% strain without observable crack formation.^[71] In contrast, HA hydrogels synthesized at 20°C exhibited brittleness and fractured under minimal deformation. Figure 11 illustrates the relationship between the nominal stress (σ_{nom}) and strain (ϵ , expressed as percentage compression) for HA cryogels synthesized at -18°C with varying concentrations of EGDE. The behavior of HA hydrogel formed at 20°C is illustrated by the filled symbols for comparison. At a stress of 3 kPa and a strain of 24%, the hydrogel failed. However, cryogels did not fail at a strain of approximately 80% under a stress of 20 to 30 kPa. Figure 12 illustrates the ability of the cryogels to withstand significant compression.^[71] When the cryogel is compressed under a piston or through manual hand pressure, it expels water, allowing for significant strain compression. Upon the release of the load, the gel sample promptly returns to its original shape through the absorption of the released water. This indicates that HA cryogels may be applicable in separation processes.

HA cryogels synthesized at -18°C demonstrated rapid deswelling and reswelling kinetics upon immersion in acetone and water, respectively.^[71] The rapid swelling and deswelling processes of HA cryogels result from their interconnected macropores, which facilitate the swift influx of water.^[72] Figure 13 shows scanning electron microscopy (SEM) and confocal laser scanning microscopy (CLSM) images of HA cryogels made at different preparation temperatures (T_{prep})^[71] The temperature during cross-linking is crucial because it affects the cryogel's microstructure. When T_{prep} is lowered from -10°C to -18°C , the average pore size decreases. Smaller spherical pores (20–40 μm) appear alongside larger pores around 100 μm .^[17] This happens because lower temperatures cause more solvent to freeze quickly, forming more ice crystals that act as templates for the pores. If T_{prep} is further lowered to -24°C , the cryogels become less interconnected and have smaller pores. This is because the structure becomes weaker at this very low temperature, causing the porous network to collapse during drying.

A novel cryogelation method has been established for producing macroporous HA cryogels, exhibiting diverse properties such as flow-dependent viscoelasticity (poroelasticity), full squeezability, and significant mechanical strength.^[73] HA cryogels were made from methacrylated

HA (meth-HA) in water at -18°C using a free-radical reaction with a redox initiator system. However, meth-HA alone could not form stable, water-insoluble cryogels, likely due to the bulky structure of HA, which limits cross-linking. When a small amount of the vinyl monomer DMAA was added, a complete gelation occurred at -18°C . This result shows the “spacer effect” of the resulting PDMAA chains, which help to connect meth-HA molecules and form a complete network, as illustrated in Figure 14.

HA cryogels in a swollen state can withstand compressive stress of up to 2.6 ± 0.2 MPa,^[73] which is approximately two orders of magnitude greater than the values achieved with the EGDE cross-linker.^[71] They demonstrate nonswelling behavior, contrasting with most hydrogels that significantly swell upon immersion in water, leading to a considerable reduction in mechanical strength (Figure 15a). The nonswelling behavior of HA cryogels is beneficial in various applications, including the regulation of network mesh size and, consequently, the controlled delivery of macromolecules.^[74–76]

HA cryogels confined between parallel plates show complete and reversible squeezability, as shown in Figure 15b.^[73] This means that water flows out of the gel's pores under high strain and flows back in when the strain is reduced. When a cryogel is compressed between the plates of a rheometer, water is expected to move out, making the gel behave more like a liquid. When the strain is lowered, the water flows back in, and the gel regains its original structure and solid-like behavior.^[77] To test this, cyclic strain-sweep experiments were performed on HA cryogels, applying strain from 1% to 1000% (γ_0) at a constant frequency of 6.3 rad/s.^[73] Figure 15c shows how the storage modulus G' (filled symbols), the loss modulus G'' (open symbols), and the loss factor $\tan \delta (= G''/G')$ (lines) change with increasing strain for a cryogel made with 5 wt% DMAA and 25% meth-HA. Circles represent increasing strain, and triangles represent decreasing strain. At around 20% strain, G'' becomes greater than G' , indicating a transition from a gel-like (solid) to a sol-like (liquid) state. However, when the strain is reduced back to 1%, the original viscoelastic properties are restored, demonstrating that this gel-to-sol transition is reversible (Figure 15c). Similar behavior was observed for cryogels made with various DMAA contents and HA methacrylation levels. This behavior confirms that the flow of water in and out of the cryogel significantly affects its viscoelastic response, a property known as

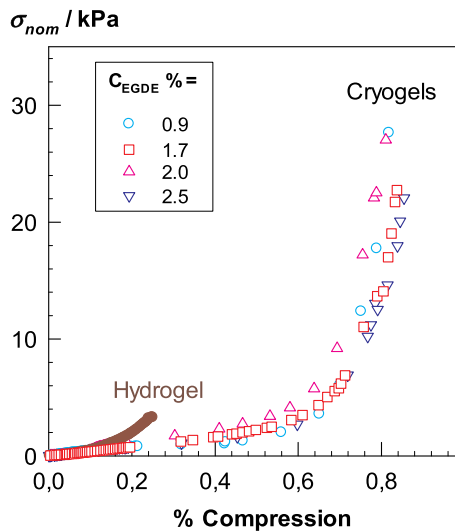


Figure 11. Stress–strain curves of HA cryogels (open symbols) and HA hydrogel (filled symbols) prepared at -18 and 20°C , respectively. HA = 7.3 wt. EGDE concentrations (C_{EGDE}) of the cryogels are indicated. The reference HA hydrogel was prepared at $C_{\text{EGDE}} = 2.5\%$.^[71]

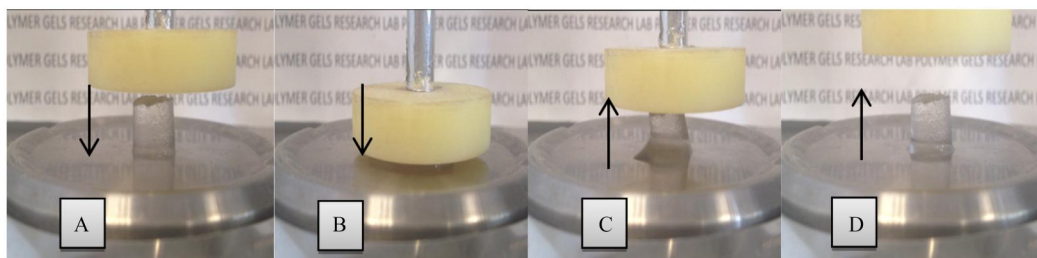


Figure 12. Photographs of a swollen HA cryogel prepared at -18°C during compression testing. The gel undergoes significant deformation under load but rapidly recovers its original shape upon load release by reabsorbing the expelled water, demonstrating excellent elasticity and reversible poroelastic behavior. HA = 7.3 wt. $C_{\text{EGDE}} = 1.7\%$.^[71]

poroelasticity.^[78–80] This is not a true breakdown of the HA network; rather, the rheometer measures the effect of water moving out of the pores, while the gel structure itself remains intact. This poroelastic behavior is similar to that of articular cartilage, a natural tissue that provides wear resistance, load support, and shock absorption in joints.^[81–84] The gel-to-sol transition in HA cryogels is important for biomedical applications, as it protects the gel structure under large strains, acting as a built-in self-defense mechanism against mechanical damage.

Cryogel composites made from HA and halloysite nanotubes (HNTs, $\text{Al}_2\text{Si}_2\text{O}_5(\text{OH})_4 \cdot n\text{H}_2\text{O}$) show enhanced mechanical strength, blood compatibility, and biocompatibility, making them promising scaffold materials for tissue engineering.^[85] HNTs are naturally occurring aluminosilicate nanoclays with a tubular structure. They typically have an outer diameter of 10–50 nm, an inner pore size of 5–20 nm, and a length of 0.5–4 μm .^[86] These nanotubes are eco-friendly, biocompatible, nontoxic, hydrophilic, and disperse well in aqueous media.^[87–89] HA/HNT composite cryogels were prepared by mixing aqueous solutions of HA and HNTs and using divinyl sulfone (DVS) as a cross-linker. Cryogelation was performed at -18°C . During freezing, ice crystals act as porogen templates, and cross-linking happens in the unfrozen regions, where HA, HNTs, and DVS are

concentrated. Figure 16a presents a schematic illustration of the formation of bare HA cryogel and HA/HNTs cryogel composites, accompanied by TEM and optical images of HNTs and the swollen cryogel composites, respectively.^[85] HNTs measure 0.5–4 μm in length and approximately 100 nm in inner diameter, exhibiting tubular structures characterized by a positively charged alumina core and a negatively charged silicate surface. Optical images of swollen cryogels reveal that bare HA cryogels appear nearly transparent. HA/HNT composites become increasingly opaque with higher HNT content, indicating better light scattering due to the nanotubes. Figure 16b presents SEM images of HA and HA/HNT cryogel composites. All cryogels exhibit macroporous structures with pore sizes from 50 to 500 μm . HA cryogels show smooth pore walls, while HA/HNT composites exhibit rougher surfaces, with roughness increasing with HNT content, likely due to nanotube accumulation on the pore walls.

Thermogravimetric analysis (TGA) shows that increasing the HNT content in HA cryogels significantly enhances their thermal stability. As the HNT content increases, weight loss at 1000°C decreases from 83% to 42%, indicating improved resistance to thermal degradation. A higher HNT content also enhances mechanical performance. For instance, at a HA:HNT weight ratio of 1:2, the Young's modulus increases from 38 ± 1 kPa to 99 ± 4 kPa, representing a 2.5-fold improvement.^[85] Beyond thermal and mechanical benefits, the inclusion of HNTs also enhances the biological performance of the cryogels, e.g., cell adhesion, proliferation, and migration are all improved, demonstrating the potential of HA–HNT composites as scaffold materials for tissue engineering.

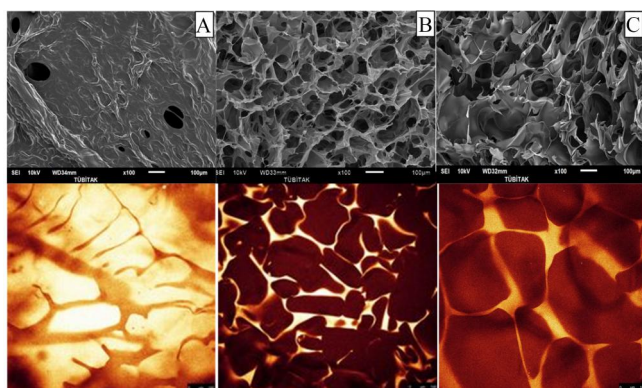


Figure 13. SEM (upper panel) and CLSM images (bottom panel) of HA cryogels formed at -24°C (A), -18°C (B), and -10°C (C). HA = 3 wt. %.^[71]

4. Future outlook: challenges and opportunities for HA-based hydrogels and cryogels

HA remains a cornerstone biomaterial for regenerative medicine and drug delivery, yet its translation into demanding biomedical applications continues to face critical challenges. Chief among these are the limited mechanical

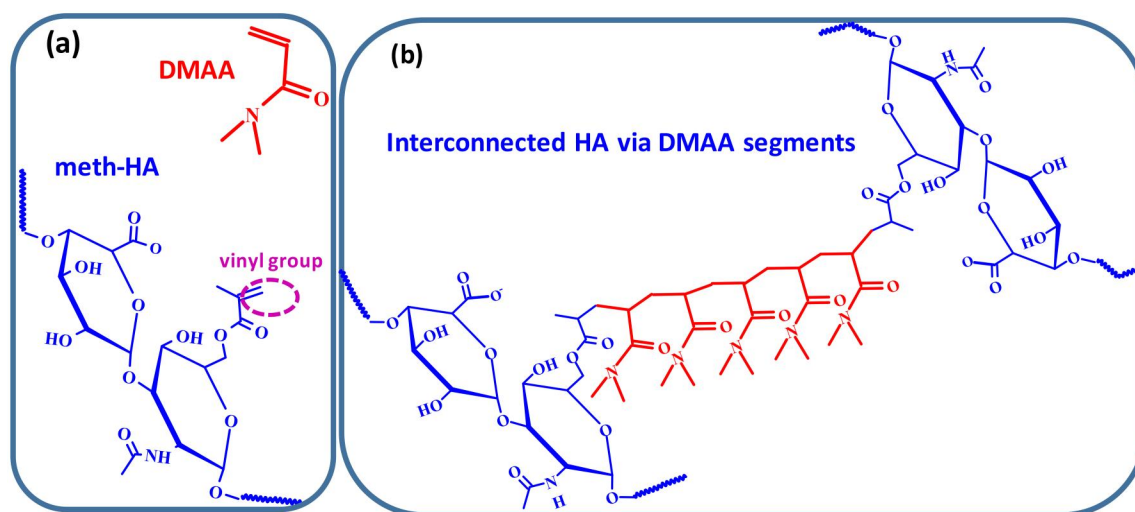


Figure 14. PDMAA and meth-HA repeat unit (highlighted in blue) before (a) and after interconnecting with PDMAA segments (b, red).^[73]

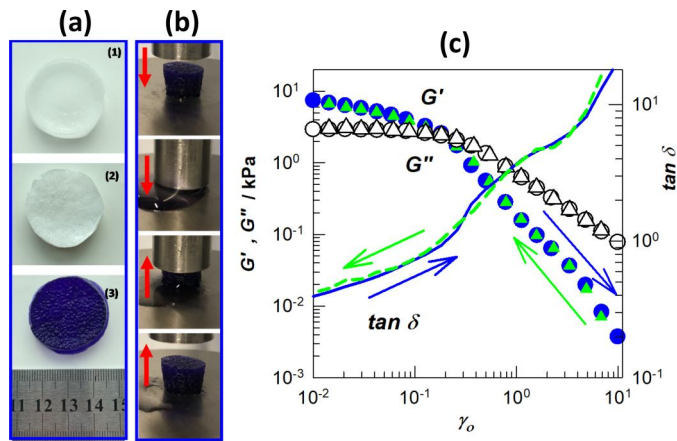


Figure 15. (a) Photographs of cryogel samples immediately after preparation (1), after freeze-drying (2), and after reaching swelling equilibrium in water, stained with crystal violet (3). All samples were synthesized with 5 wt% DMAA and 25% meth-HA. (b) Compression–recovery test images of a cryogel under cyclic loading and unloading up to 90% strain, indicated by down and up arrows, respectively. Composition: 5 wt% DMAA, 25% meth-HA. (c) Rheological behavior of a cryogel specimen (5 wt% DMAA, 25% meth-HA) showing G' (filled symbols), G'' (open symbols), and $\tan \delta$ (lines) as a function of strain amplitude (γ_0) at a frequency of $\omega = 6.3$ rad/s. Up and down strain sweep tests are represented by circles and triangles, respectively, while $\tan \delta$ is shown by solid (up) and dashed (down) lines. Temperature = 25 °C.^[73]

robustness of conventional HA hydrogels, their susceptibility to rapid enzymatic degradation *in vivo*, and the difficulty of balancing high water content with load-bearing capacity. While strategies such as double- and triple-network architectures and cryogelation have markedly enhanced mechanical resilience, their reproducibility, scalability, and precise control over structural heterogeneity remain significant hurdles for clinical implementation. Another pressing limitation is the immune response and biodegradation kinetics of chemically modified HA, which must be optimized to achieve predictable performance across different tissue environments.

At the same time, HA-based hydrogels and cryogels offer substantial opportunities that position them at the forefront of next-generation biomaterials. The tunability of HA chemistry enables modular design for targeted mechanical and biological functions, while DN and TN architectures open pathways toward implants capable of withstanding physiologically relevant stresses. Cryogels, with their macroporosity, poroelastic behavior, and reversible squeezability, provide unique advantages for dynamic tissue environments, particularly in load-bearing tissues such as cartilage and intervertebral disks. Furthermore, their nonswelling behavior and controllable pore architecture make them attractive for localized, sustained drug delivery and cell migration scaffolds.

Looking forward, the integration of HA hydrogels and cryogels with emerging technologies such as 3D/4D printing, biofabrication, and nanomaterial reinforcement presents transformative opportunities. Multi-scale structural design could yield biomaterials that replicate both the viscoelasticity and adaptive remodeling of native extracellular matrix. In parallel, bioorthogonal and enzymatically cleavable cross-linking chemistries offer prospects for achieving both mechanical integrity and controlled biodegradation. Ultimately, the successful convergence of these approaches will

determine whether HA-based hydrogels and cryogels can transition from promising laboratory materials to reliable clinical platforms for load-bearing tissue repair, long-term drug delivery, and dynamic biomedical devices.

5. Conclusions

Hyaluronic acid (HA) is a naturally occurring glycosaminoglycan that plays a pivotal role in the extracellular matrix (ECM) of connective tissues, contributing to hydration, lubrication, and biomechanical integrity. First described in 1880 as “hyalomucin” by Portes and later isolated in pure form from bovine vitreous bodies by Meyer and Palmer in 1934, HA has since become a cornerstone material in biomedical and pharmaceutical applications. Its exceptional water-binding capacity, biocompatibility, and immunomodulatory properties have led to widespread use in joint lubrication, wound healing, ophthalmology, and drug delivery. Industrial production, largely *via* *Streptococcus* fermentation, has facilitated its availability for diverse applications.

Despite these advantages, native HA and its chemically cross-linked hydrogels exhibit intrinsic limitations, particularly poor mechanical strength and rapid *in vivo* degradation, restricting their utility in load-bearing or long-term biomedical applications. These shortcomings stem from the inability of conventional HA networks to dissipate mechanical energy effectively, causing structural failure under relatively low stress. Conventional strategies for HA hydrogel synthesis typically involve cross-linking through its carboxyl, hydroxyl, or acetamido groups, using agents such as bisepoxides or divinylsulfone. While such methods improve stability, they often fail to achieve the mechanical robustness required for advanced applications.

This work first reviews these traditional cross-linking strategies, highlighting their benefits and limitations. It then focuses on recent developments, many originating from our laboratory, that address these challenges through innovative network architectures. In particular, the double-network (DN) approach and the cryogelation technology are discussed in detail. Table 1 compiles the mechanical properties of hydrogels and cryogels based on HA. It was shown that the fracture stress and fracture strain of HA hydrogel increase dramatically from 0.03 MPa to 12.2 MPa and from 40% to 94%, respectively, upon formation of the double-network structure. Triple-network hydrogels synthesized from DN hydrogels can endure compressive loads ranging from 10 to 22 MPa at 95% compression and demonstrate a Young’s modulus E of up to 1 MPa. The values presented represent the maximum fracture stresses for HA hydrogels documented in the existing literature. The development of TN hydrogels based on HA marks a notable progression in HA hydrogel research, with prospective applications in load-bearing biomedical contexts. Moreover, ECM-inspired hydrogels made of meth-HA and meth-SF contain highly elastic polymer chains characterized by high compressibility and extensibility. They exhibit a Young’s modulus of up to 36 kPa, a fracture stress of 4.2 MPa and 15 kPa in

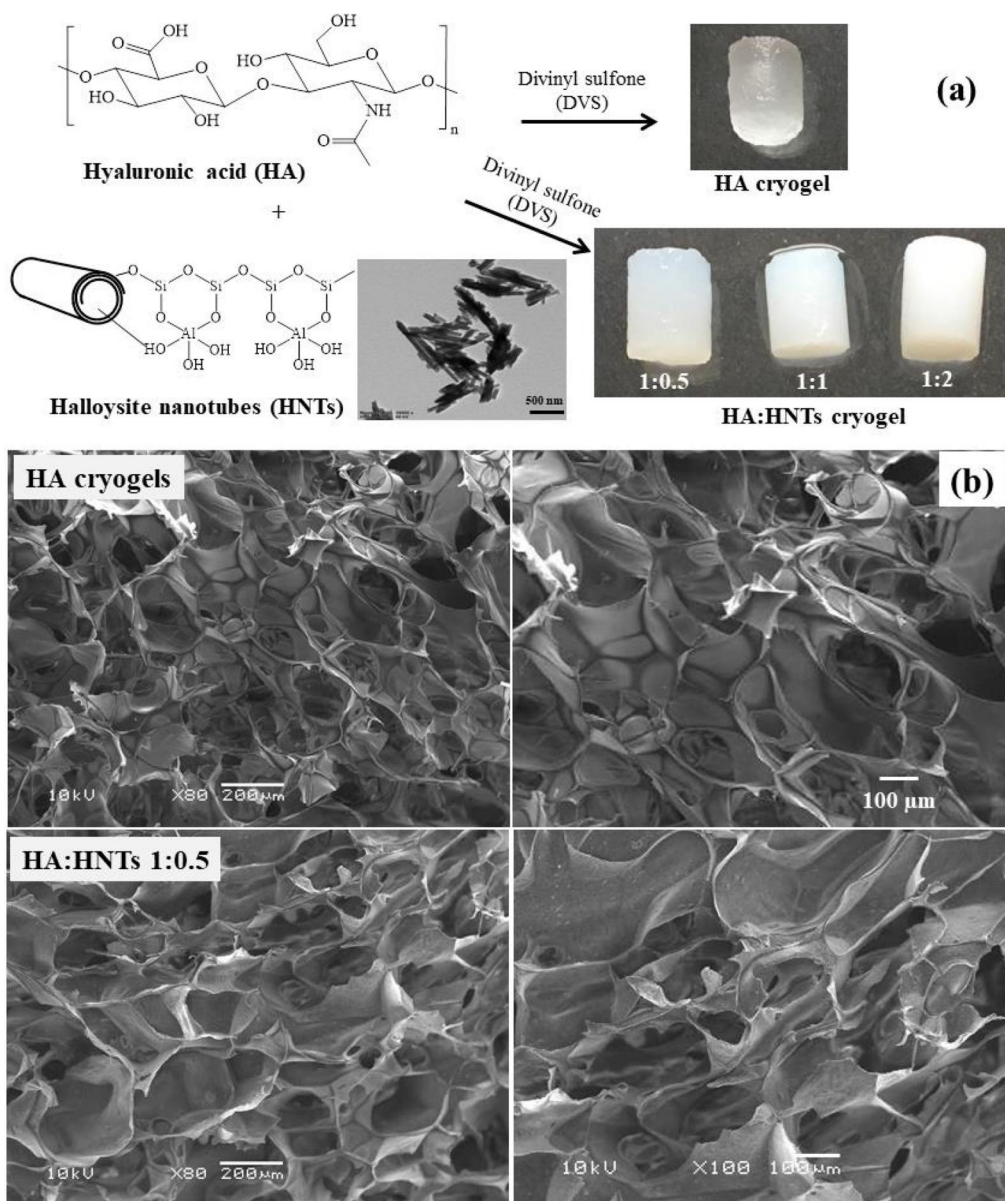


Figure 16. (a) Schematic illustration of formation of bare HA cryogel and HA/HNTs cryogel composites together with the TEM and optical images of HNTs and swollen cryogel composites, respectively. (b) SEM images of HA (upper panel) and HA/HNT composite at 1:0.5 weight ratio (b).^[85]

Table 1. Mechanical properties of hydrogels and cryogels based on HA.

Hydrogel/cryogel type	Compressive modulus	Compressive stress	Compressive strain	Ref.
Meth-HA/DMAA TN hydrogel	1.0 MPa	22 MPa	95%	[43]
HA/DMAA/EGDE DN hydrogel	1.0 MPa	19 MPa	90%	[56]
Meth-HA/DMAA DN hydrogel	0.6 MPa	12 MPa	94%	[43]
Meth-HA/DMAA DN hydrogel	0.5 MPa	5.2 MPa	87%	[58]
Meth-HA/meth-SF DN hydrogel	36 kPa	4.2 MPa (15 kPa elongation)	60%	[59]
Meth-HA/DMAA cryogel	–	2.6 MPa	300% elongation >99%	[73]
HA/HNTs cryogel	99 kPa	0.6 MPa	>99%	[85]
HA/EGDE cryogel	–	30 kPa	80%	[71]

compression and tensile tests, and they can be compressed up to 60% and stretched up to 300%.

Macroporous HA cryogels developed by the cryogelation strategy exhibit diverse properties such as flow-dependent viscoelasticity (poroelasticity), full squeezability, and significant mechanical strength. When swollen in water, the cryogels can withstand compressive stress of up to 2.6 ± 0.2 MPa

and exhibit nonswelling behavior, which is beneficial in various applications, including the regulation of network mesh size and, consequently, the controlled delivery of macromolecules. Another characteristic of HA cryogels is their reversible squeezability, meaning that water flows out of the gel's pores under high strain and flows back in when the strain is reduced. This behavior also confirms that the flow of water

in and out of the cryogel significantly affects its viscoelastic response, a property known as poroelasticity. This poroelastic behavior is similar to that of articular cartilage, a natural tissue that provides wear resistance, load support, and shock absorption in joints. The gel-to-sol transition in HA cryogels is important for biomedical applications, as it protects the gel structure under large strains, acting as a built-in self-defense mechanism against mechanical damage.

The double-network and cryogelation strategies have been adapted to HA to produce hydrogels that are not only biocompatible and stable but also capable of withstanding significant mechanical stress, thereby expanding their potential in surgical interventions, load-bearing tissue engineering, and controlled drug delivery. The combination of HA's inherent biological advantages with mechanically resilient architectures offers a promising path toward next-generation biomaterials.

Acknowledgment

O.O. thanks the Turkish Academy of Sciences (TUBA) for the partial support.

Disclosure statement

No potential conflict of interest was reported by the author(s).

Funding

This work was supported by Türkiye Bilimler Akademisi.

References

- [1] Khunmanee, S.; Jeong, Y.; Park, H. Crosslinking Method of Hyaluronic-Based Hydrogel for Biomedical Applications. *J. Tissue Eng.* **2017**, *8*, 1–16.
- [2] Boeriu, C. G.; Springer, J.; Kooy, F. K.; van den Broek, L. A. M.; Eggink, G. Production Methods for Hyaluronan. *Int. J. Carbohydr. Chem.* **2013**, *2013*, 1–14. DOI: [10.1155/2013/624967](https://doi.org/10.1155/2013/624967).
- [3] Fallacara, A.; Baldini, E.; Manfredini, S.; Vertuani, S. Hyaluronic Acid in the Third Millennium. *Polymers* **2018**, *10*, 701. DOI: [10.3390/polym10070701](https://doi.org/10.3390/polym10070701).
- [4] Meyer, K.; Palmer, J. W. The Polysaccharide of the Vitreous Humor. *J. Biol. Chem.* **1934**, *107*, 629–634. DOI: [10.1016/S0021-9258\(18\)75338-6](https://doi.org/10.1016/S0021-9258(18)75338-6).
- [5] Mihajlovic, M.; Fermin, L.; Ito, K.; van Nostrum, C. F.; Vermonden, T. Hyaluronic Acid-Based Supramolecular Hydrogels for Biomedical Applications. *Multifunct. Mater.* **2021**, *4*, 032001. DOI: [10.1088/2399-7532/ac1c8a](https://doi.org/10.1088/2399-7532/ac1c8a).
- [6] Wei, M.; Huang, Y.; Zhu, J.; Qiao, Y.; Xiao, N.; Jin, M.; Gao, H.; Huang, Y.; Hu, X.; Li, O. Advances in Hyaluronic Acid Production: Biosynthesis and Genetic Engineering Strategies Based on Streptococcus—A Review. *Int. J. Biol. Macromol.* **2024**, *270*, 132334. DOI: [10.1016/j.ijbiomac.2024.132334](https://doi.org/10.1016/j.ijbiomac.2024.132334).
- [7] Burdick, J. A.; Prestwich, G. D. Hyaluronic Acid Hydrogels for Biomedical Applications. *Adv. Mater.* **2011**, *23*, H41–H56. DOI: [10.1002/adma.201003963](https://doi.org/10.1002/adma.201003963).
- [8] Collins, M. N.; Birkinshaw, C. Physical Properties of Crosslinked Hyaluronic Acid Hydrogels. *J. Mater. Sci. Mater. Med.* **2008**, *19*, 3335–3343. DOI: [10.1007/s10856-008-3476-4](https://doi.org/10.1007/s10856-008-3476-4).
- [9] Singh, S.; Rai, A. K.; Tewari, R. P. Recent Advancement in Hyaluronic Acid-Based Hydrogel for Biomedical Engineering Application: A Mini-Review. *Mater. Today: Proc.* **2023**, *78*, 138–144. DOI: [10.1016/j.matpr.2022.12.208](https://doi.org/10.1016/j.matpr.2022.12.208).
- [10] Xu, X.; Jha, A. K.; Harrington, D. A.; Farach-Carson, M. C.; Jia, X. Hyaluronic Acid-Based Hydrogels: From a Natural Polysaccharide to Complex Networks. *Soft Matter* **2012**, *8*, 3280–3294. DOI: [10.1039/C2SM06463D](https://doi.org/10.1039/C2SM06463D).
- [11] Yasin, A.; Ren, Y.; Li, J.; Sheng, Y.; Cao, J.; Zhang, K. Advances in Hyaluronic Acid for Biomedical Applications. *Front. Bioeng. Biotechnol.* **2022**, *10*, 910290. DOI: [10.3389/fbioe.2022.910290](https://doi.org/10.3389/fbioe.2022.910290).
- [12] Brown, H. R. A Model of the Fracture of Double Network Gels. *Macromolecules* **2007**, *40*, 3815–3818. DOI: [10.1021/ma062642y](https://doi.org/10.1021/ma062642y).
- [13] Abdurrahmanoglu, S.; Can, V.; Okay, O. Design of High-Toughness Polyacrylamide Hydrogels by Hydrophobic Modification. *Polymer* **2009**, *50*, 5449–5455. DOI: [10.1016/j.polymer.2009.09.042](https://doi.org/10.1016/j.polymer.2009.09.042).
- [14] Gong, J. P.; Katsuyama, Y.; Kurokawa, T.; Osada, Y. Double-Network Hydrogels with Extremely High Mechanical Strength. *Adv. Mater.* **2003**, *15*, 1155–1158. DOI: [10.1002/adma.200304907](https://doi.org/10.1002/adma.200304907).
- [15] Tanaka, Y.; Gong, J. P.; Osada, Y. Novel Hydrogels with Excellent Mechanical Performance. *Prog. Polym. Sci.* **2005**, *30*, 1–9. DOI: [10.1016/j.progpolymsci.2004.11.003](https://doi.org/10.1016/j.progpolymsci.2004.11.003).
- [16] Lozinsky, V. I.; Okay, O. Basic Principles of Cryotropic Gelation. *Adv. Polym. Sci.* **2014**, *263*, 49–102.
- [17] Okay, O.; Lozinsky, V. I. Synthesis and Structure–Property Relationships of Cryogels. *Adv. Polym. Sci.* **2014**, *263*, 103–157.
- [18] Luo, Y.; Tan, J.; Zhou, Y.; Guo, Y.; Liao, X.; He, L.; Li, D.; Li, X.; Liu, Y. From Crosslinking Strategies to Biomedical Applications of Hyaluronic Acid-Based Hydrogels: A Review. *Int. J. Biol. Macromol.* **2023**, *231*, 123308. DOI: [10.1016/j.ijbiomac.2023.123308](https://doi.org/10.1016/j.ijbiomac.2023.123308).
- [19] Gholamali, I.; Vu, T. T.; Jo, S.-H.; Park, S. H.; Lim, K. T. Exploring the Progress of Hyaluronic Acid Hydrogels: Synthesis, Characteristics, and Wide-Ranging Applications. *Materials* **2024**, *17*, 2439. DOI: [10.3390/ma17102439](https://doi.org/10.3390/ma17102439).
- [20] Schanté, C. E.; Zuber, G.; Herlin, C.; Vandamme, T. F. Chemical Modifications of Hyaluronic Acid for the Synthesis of Derivatives for a Broad Range of Biomedical Applications. *Carbohydr. Polym.* **2011**, *85*, 469–489. DOI: [10.1016/j.carbpol.2011.03.019](https://doi.org/10.1016/j.carbpol.2011.03.019).
- [21] Degirmenci, A.; Sanyal, R.; Sanyal, A. Metal-Free Click-Chemistry: A Powerful Tool for Fabricating Hydrogels for Biomedical Applications. *Bioconjug. Chem.* **2024**, *35*, 433–452. DOI: [10.1021/acs.bioconjchem.4c00003](https://doi.org/10.1021/acs.bioconjchem.4c00003).
- [22] Faivre, J.; Pigweh, A. I.; Iehl, J.; Maffert, P.; Goekjian, P.; Bourdon, P. Crosslinking Hyaluronic Acid Soft-Tissue Fillers: Current Status and Perspectives from an Industrial Point of View. *Expert Rev. Med. Devices* **2021**, *18*, 1175–1187. DOI: [10.1080/17434440.2021.2014320](https://doi.org/10.1080/17434440.2021.2014320).
- [23] Ranga, A.; Lutolf, M. P.; Hilborn, J.; Ossipov, D. A. Hyaluronic Acid Hydrogels Formed in Situ by Transglutaminase Catalyzed Reaction. *Biomacromolecules* **2016**, *17*, 1553–1560. DOI: [10.1021/acs.biomac.5b01587](https://doi.org/10.1021/acs.biomac.5b01587).
- [24] Brogiere, N.; Isenmann, L.; Zenobi-Wong, M. Novel Enzymatically Cross-Linked Hyaluronan Hydrogels Support the Formation of 3D Neuronal Networks. *Biomaterials* **2016**, *99*, 47–55. DOI: [10.1016/j.biomaterials.2016.04.036](https://doi.org/10.1016/j.biomaterials.2016.04.036).
- [25] Bas, Y.; Sanyal, R.; Sanyal, A. Hyaluronic-Acid Based Redox-Responsive Hydrogels Using the Diels-Alder Reaction for on-Demand Release of Biomacromolecules. *J. Macromol. Sci. A* **2023**, *60*, 246–254. DOI: [10.1080/10601325.2023.2190357](https://doi.org/10.1080/10601325.2023.2190357).
- [26] Yu, F.; Cao, X.; Du, J.; Wang, G.; Chen, X. Multifunctional Hydrogel with Good Structure Integrity, Self-Healing, and Tissue Adhesive Property Formed by Combining Diels-Alder Click Reaction and Acylhydrazone Bond. *ACS Appl. Mater. Interfaces* **2015**, *7*, 24023–24031. DOI: [10.1021/acsami.5b06896](https://doi.org/10.1021/acsami.5b06896).
- [27] Lee, H. J.; Fernandes-Cunha, G. M.; Myung, D. In Situ Forming Hyaluronic Acid Hydrogel through Visible Light-Induced Thiol Ene Reaction. *React. Funct. Polym.* **2018**, *131*, 29–35. DOI: [10.1016/j.reactfunctpolym.2018.06.010](https://doi.org/10.1016/j.reactfunctpolym.2018.06.010).

- [28] Hozumi, T.; Kageyama, T.; Ohta, S.; Fukuda, J.; Ito, T. Injectable Hydrogel with Slow Degradability Composed of Gelatin and Hyaluronic Acid Cross-Linked by Schiff's Base Formation. *Biomacromolecules* **2018**, *19*, 288–297. DOI: [10.1021/acs.biomac.7b01133](https://doi.org/10.1021/acs.biomac.7b01133).
- [29] Yeingst, T. J.; Helton, A. M.; Hayes, D. J. Applications of Diels–Alder Chemistry in Biomaterials and Drug Delivery. *Macromol. Biosci.* **2024**, *24*, e2400274. DOI: [10.1002/mabi.202400274](https://doi.org/10.1002/mabi.202400274).
- [30] Segura, T.; Anderson, B. C.; Chung, P. H.; Webber, R. E.; Shull, K. R.; Shea, L. D. Crosslinked Hyaluronic Acid Hydrogels: A Strategy to Functionalize and Pattern. *Biomaterials* **2005**, *26*, 359–371. DOI: [10.1016/j.biomaterials.2004.02.067](https://doi.org/10.1016/j.biomaterials.2004.02.067).
- [31] Xue, Y.; Chen, H.; Xu, C.; Yu, D.; Xu, H.; Hu, Y. Synthesis of Hyaluronic Acid Hydrogels by Crosslinking the Mixture of High-Molecular-Weight Hyaluronic Acid and Low-Molecular-Weight Hyaluronic Acid with 1,4-Butanediol Diglycidyl Ether. *RSC Adv.* **2020**, *10*, 7206–7213. DOI: [10.1039/c9ra09271d](https://doi.org/10.1039/c9ra09271d).
- [32] Lai, J.-Y. Relationship between Structure and Cytocompatibility of Divinyl Sulfone Cross-Linked Hyaluronic Acid. *Carbohydr. Polym.* **2014**, *101*, 203–212. DOI: [10.1016/j.carbpol.2013.09.060](https://doi.org/10.1016/j.carbpol.2013.09.060).
- [33] del Olmo, J. A.; Alonso, J. M.; Martínez, V. S.; Ruiz-Rubio, L.; González, R. P.; Vilas-Vilela, J. L.; Pérez-Álvarez, L. Biocompatible Hyaluronic Acid-Divinyl Sulfone Injectable Hydrogels for Sustained Drug Release with Enhanced Antibacterial Properties against *Staphylococcus aureus*. *Mater. Sci. Eng. C* **2021**, *125*, 112102.
- [34] Tomihata, K.; Ikada, Y. Crosslinking of Hyaluronic Acid with Glutaraldehyde. *J. Polym. Sci. A Polym. Chem.* **1997**, *35*, 3553–3559. DOI: [10.1002/\(SICI\)1099-0518\(19971130\)35:16<3553::AID-POLA22>3.0.CO;2-D](https://doi.org/10.1002/(SICI)1099-0518(19971130)35:16<3553::AID-POLA22>3.0.CO;2-D).
- [35] Tomihata, K.; Ikada, Y. Crosslinking of Hyaluronic Acid with Water-Soluble Carbodiimide. *J. Biomed. Mater. Res.* **1997**, *37*, 243–251. DOI: [10.1002/\(SICI\)1097-4636\(199711\)37:2<243::AID-JBM14>3.3.CO;2-V](https://doi.org/10.1002/(SICI)1097-4636(199711)37:2<243::AID-JBM14>3.3.CO;2-V).
- [36] Chen, Y.-H.; Li, J.; Hao, Y.-B.; Qi, J. X.; Dong, N.-G.; Wu, C.-L.; Wang, Q. Preparation and Characterization of Composite Hydrogels Based on Crosslinked Hyaluronic Acid and Sodium Alginate. *J. Appl. Polym. Sci.* **2015**, *132*, 41898.
- [37] Litwiniuk, M.; Krejner, A.; Speyrer, M. S.; Gauto, A. R.; Grzela, T. Hyaluronic Acid in Inflammation and Tissue Regeneration. *Wounds* **2016**, *28*, 78–88.
- [38] Su, W.-Y.; Chen, K.-H.; Chen, Y.-C.; Lee, Y.-H.; Tseng, C.-L.; Lin, F.-H. An Injectable Oxidated Hyaluronic Acid/Adipic Acid Dihydrazide Hydrogel as a Vitreous Substitute. *J. Biomater. Sci. Polym. Ed.* **2011**, *22*, 1777–1797. DOI: [10.1163/092050610X522729](https://doi.org/10.1163/092050610X522729).
- [39] Wang, L.-S.; Lee, F.; Lim, J.; Du, C.; Wan, A. C. A.; Lee, S. S.; Kurisawa, M. Enzymatic Conjugation of a Bioactive Peptide into an Injectable Hyaluronic Acid–Tyramine Hydrogel System to Promote the Formation of Functional Vasculature. *Acta Biomater.* **2014**, *10*, 2539–2550. DOI: [10.1016/j.actbio.2014.02.022](https://doi.org/10.1016/j.actbio.2014.02.022).
- [40] Leach, J. B.; Bivens, K. A.; Patrick, C. W.; Schmidt, C. E. Photocrosslinked Hyaluronic Acid Hydrogels: Natural, Biodegradable Tissue Engineering Scaffolds. *Biotechnol. Bioeng* **2003**, *82*, 578–589.
- [41] Prado, S. S.; Weaver, J. M.; Love, B. J. Gelation of Photopolymerized Hyaluronic Acid Grafted with Glycidyl Methacrylate. *Mater. Sci. Eng. C* **2011**, *31*, 1767–1771. DOI: [10.1016/j.msec.2011.08.008](https://doi.org/10.1016/j.msec.2011.08.008).
- [42] Ibrahim, S.; Kothapalli, C. R.; Kang, Q. K.; Ramamurthi, A. Characterization of Glycidyl Methacrylate– Crosslinked Hyaluronan Hydrogel Scaffolds Incorporating Elastogenic Hyaluronan Oligomers. *Acta Biomater.* **2011**, *7*, 653–665. DOI: [10.1016/j.actbio.2010.08.006](https://doi.org/10.1016/j.actbio.2010.08.006).
- [43] Tavsanlı, B.; Can, V.; Okay, O. Mechanically Strong Triple Network Hydrogels Based on Hyaluronan and Poly(N,N-Dimethylacrylamide). *Soft Matter* **2015**, *11*, 8517–8524. DOI: [10.1039/c5sm01941a](https://doi.org/10.1039/c5sm01941a).
- [44] Ye, X.; Li, X.; Shen, Y.; Chang, G.; Yang, J.; Gu, Z. Self-Healing pH-Sensitive Cytosine- and Guanosine-Modified Hyaluronic Acid Hydrogels via Hydrogen Bonding. *Polymer* **2017**, *108*, 348–360. DOI: [10.1016/j.polymer.2016.11.063](https://doi.org/10.1016/j.polymer.2016.11.063).
- [45] Chen, X.; Liu, Z. A pH-Responsive Hydrogel Based on a Tumor-Targeting Mesoporous Silica Nanocomposite for Sustained Cancer Labeling and Therapy. *Macromol. Rapid Commun.* **2016**, *37*, 1533–1539. DOI: [10.1002/marc.201600261](https://doi.org/10.1002/marc.201600261).
- [46] Zhang, F.; Wu, J.; Kang, D.; Zhang, H. Development of a Complex Hydrogel of Hyaluronan and PVA Embedded with Silver Nanoparticles and Its Facile Studies on *Escherichia coli*. *J. Biomater. Sci. Polym. Ed.* **2013**, *24*, 1410–1425. DOI: [10.1080/09205063.2012.763109](https://doi.org/10.1080/09205063.2012.763109).
- [47] Shin, M.; Galarraga, J. H.; Kwon, M. Y.; Lee, H.; Burdick, J. A. Gallol-Derived ECM-Mimetic Adhesive Bioinks Exhibiting Temporal Shear-Thinning and Stabilization Behavior. *Acta Biomater.* **2019**, *95*, 165–175. DOI: [10.1016/j.actbio.2018.10.028](https://doi.org/10.1016/j.actbio.2018.10.028).
- [48] Hirokawa, T.; Tanaka, T. J. Volume Phase Transition in a Nonionic Gel. *J. Chem. Phys.* **1984**, *81*, 6379–6380. DOI: [10.1063/1.447548](https://doi.org/10.1063/1.447548).
- [49] Gundogan, N.; Melekaslan, D.; Okay, O. Rubber Elasticity of Poly(N-Isopropylacrylamide) Gels at Various Charge Densities. *Macromolecules* **2002**, *35*, 5616–5622. DOI: [10.1021/ma020151h](https://doi.org/10.1021/ma020151h).
- [50] Chou, P.-Y.; Chen, S. H.; Chen, C.-H.; Chen, S.-H.; Fong, Y.-T.; Chen, J. P. Thermo-Responsive in-Situ Forming Hydrogels as Barriers to Prevent Post-Operative Peritendinous Adhesion. *Acta Biomater.* **2017**, *63*, 85–95. DOI: [10.1016/j.actbio.2017.09.010](https://doi.org/10.1016/j.actbio.2017.09.010).
- [51] Tabet, A.; Park, J. Y.; Shilts, J.; Sokolowski, K.; Rana, V. K.; Kamp, M.; Warner, N.; Hoogland, D.; Scherman, O. A. Protein-Mediated Gelation and Nano-Scale Assembly of Unfunctionalized Hyaluronic Acid and Chondroitin Sulfate. *Fl000 Res.* **2018**, *7*, 1827.
- [52] Lu, K. Y.; Lin, Y. C.; Lu, H. T.; Ho, Y. C.; Weng, S. C.; Tsai, M. L.; Mi, F. L. A Novel Injectable in Situ Forming Gel Based on Carboxymethyl Hexanoyl Chitosan/Hyaluronic Acid Polymer Blending for Sustained Release of Berberine. *Carbohydr. Polym.* **2019**, *206*, 664–673. DOI: [10.1016/j.carbpol.2018.11.050](https://doi.org/10.1016/j.carbpol.2018.11.050).
- [53] Miyazaki, T.; Yomota, C.; Okada, S. Development and Release Characterization of Hyaluronan–Doxycycline Gels Based on Metal Coordination. *J. Control. Release* **2001**, *76*, 337–347. DOI: [10.1016/s0168-3659\(01\)00453-9](https://doi.org/10.1016/s0168-3659(01)00453-9).
- [54] Nakaji-Hirabayashi, T.; Kato, K.; Iwata, H. Hyaluronic Acid Hydrogel Loaded with Genetically-Engineered Brain-Derived Neurotrophic Factor as a Neural Cell Carrier. *Biomaterials* **2009**, *30*, 4581–4589. DOI: [10.1016/j.biomaterials.2009.05.009](https://doi.org/10.1016/j.biomaterials.2009.05.009).
- [55] Shi, L.; Han, Y.; Hilborn, J.; Ossipov, D. ‘Smart’ Drug Loaded Nanoparticle Delivery from a Self-Healing Hydrogel Enabled by Dynamic Magnesium-Biopolymer Chemistry. *Chem. Commun.* **2016**, *52*, 11151–11154. DOI: [10.1039/c6cc05565f](https://doi.org/10.1039/c6cc05565f).
- [56] Tavsanlı, B.; Okay, O. Preparation and Fracture Process of High Strength Hyaluronic Acid Hydrogels Cross-Linked by Ethylene Glycol Diglycidyl Ether. *React. Funct. Polym.* **2016**, *109*, 42–51. DOI: [10.1016/j.reactfunctpolym.2016.10.001](https://doi.org/10.1016/j.reactfunctpolym.2016.10.001).
- [57] Gong, J. P. Why Are Double Network Hydrogels so Tough? *Soft Matter* **2010**, *6*, 2583–2590. DOI: [10.1039/b924290b](https://doi.org/10.1039/b924290b).
- [58] Weng, L.; Gouldstone, A.; Wu, Y.; Chen, W. Mechanically Strong Double Network Photocrosslinked Hydrogels from N,N-Dimethylacrylamide and Glycidyl Methacrylated Hyaluronan. *Biomaterials* **2008**, *29*, 2153–2163. DOI: [10.1016/j.biomaterials.2008.01.012](https://doi.org/10.1016/j.biomaterials.2008.01.012).
- [59] Yetiskin, B.; Tavsanlı, B.; Okay, O. Photocurable Methacrylated Silk Fibroin/Hyaluronic Acid Dual Macrocrosslinker System Generating Extracellular Matrix-Inspired Tough and Stretchable Hydrogels. *Macromol. Mater. Eng.* **2022**, *307*, 2200334.
- [60] Lozinsky, V. I.; Vainerman, E. S.; Titova, E. F.; Belavtseva, E. M.; Rogozhin, S. V. Study of Cryostructurization of Polymer Systems IV. Cryostructurization of the System: Solvent—Vinyl Monomer—Divinyl Monomer—Initiator of Polymerization.

- Colloid Polym Sci.* **1984**, 262, 769–774. DOI: [10.1007/BF01451705](https://doi.org/10.1007/BF01451705).
- [61] Lozinsky, V. I. Cryogels on the Basis of Natural and Synthetic Polymers: Preparation, Properties and Application. *Russ. Chem. Rev.* **2002**, 71, 489–511. DOI: [10.1070/RC2002v071n06ABEH000720](https://doi.org/10.1070/RC2002v071n06ABEH000720).
- [62] Okay, O. Cryogelation Reactions and Cryogels: Principles and Challenges. *Turk. J. Chem.* **2023**, 47, 910–926. DOI: [10.55730/1300-0527.3586](https://doi.org/10.55730/1300-0527.3586).
- [63] Mattiasson, B.; Kumar, A.; Galaev, I. Y. *Macroporous Polymers: Production, Properties and Biotechnological/Biomedical Applications*; CRC Press: New York, 2010.
- [64] Henderson, T. M. A.; Ladewig, K.; Haylock, D. N.; McLean, K. M.; O'Connor, A. J. Cryogels for Biomedical Applications. *J. Mater. Chem. B* **2013**, 1, 2682–2695. DOI: [10.1039/c3tb20280a](https://doi.org/10.1039/c3tb20280a).
- [65] Doser, G.; Su, E.; Okay, O. Effects of Cryogenic Condition and Chemistry on the Properties of Synthetic and Biopolymer Cryogels. *React. Funct. Polym.* **2023**, 190, 105635. DOI: [10.1016/j.reactfunctpolym.2023.105635](https://doi.org/10.1016/j.reactfunctpolym.2023.105635).
- [66] Ozmen, M. M.; Okay, O. Superfast Responsive Ionic Hydrogels with Controllable Pore Size. *Polymer* **2005**, 46, 8119–8127. DOI: [10.1016/j.polymer.2005.06.102](https://doi.org/10.1016/j.polymer.2005.06.102).
- [67] Baimenov, A.; Berillo, D. A.; Pouloupoulos, S. G.; Inglezakis, V. J. A Review of Cryogels Synthesis, Characterization and Applications on the Removal of Heavy Metals from Aqueous Solutions. *Adv. Colloid Interface Sci.* **2020**, 276, 102088. DOI: [10.1016/j.cis.2019.102088](https://doi.org/10.1016/j.cis.2019.102088).
- [68] Okay, O. *Polymeric Cryogels. Macroporous Gels with Remarkable Properties*; Springer International Publishing: Switzerland **2014**.
- [69] Bakhshpour, M.; Idil, N.; Perçin, I.; Denizli, A. Biomedical Applications of Polymeric Cryogels. *Appl. Sci.* **2019**, 9, 553. DOI: [10.3390/app9030553](https://doi.org/10.3390/app9030553).
- [70] Muslumova, S.; Yetiskin, B.; Okay, O. Highly Stretchable and Rapid Self-Recoverable Cryogels Based on Butyl Rubber as Reusable Sorbent. *Gels* **2019**, 5, 1. DOI: [10.3390/gels5010001](https://doi.org/10.3390/gels5010001).
- [71] Strom, A.; Larsson, A.; Okay, O. Preparation and Physical Properties of Hyaluronic Acid-Based Cryogels. *J. Appl. Polym. Sci.* **2015**, 132, 42194.
- [72] Dinu, M. V.; Ozmen, M. M.; Dragan, E. S.; Okay, O. Freezing as a Path to Built Macroporous Structures: Superfast Responsive Polyacrylamide Hydrogels. *Polymer* **2007**, 48, 195–204. DOI: [10.1016/j.polymer.2006.11.022](https://doi.org/10.1016/j.polymer.2006.11.022).
- [73] Tavsanlı, B.; Okay, O. Macroporous Methacrylated Hyaluronic Acid Cryogels of High Mechanical Strength and Flow-Dependent Viscoelasticity. *Carbohydr. Polym.* **2020**, 229, 115458. DOI: [10.1016/j.carbpol.2019.115458](https://doi.org/10.1016/j.carbpol.2019.115458).
- [74] Truong, V. X.; Tsang, K. M.; Forsythe, J. S. Nonswelling Click Cross-Linked Gelatin and PEG Hydrogels with Tunable Properties Using Pluronic Linkers. *Biomacromolecules* **2017**, 18, 757–766. DOI: [10.1021/acs.biomac.6b01601](https://doi.org/10.1021/acs.biomac.6b01601).
- [75] Ding, H.; Li, B.; Liu, Z.; Liu, G.; Pu, S.; Feng, Y.; Jia, D.; Zhou, Y. Nonswelling Injectable Chitosan Hydrogel via UV Crosslinking Induced Hydrophobic Effect for Minimally Invasive Tissue Engineering. *Carbohydr. Polym.* **2021**, 252, 117143. DOI: [10.1016/j.carbpol.2020.117143](https://doi.org/10.1016/j.carbpol.2020.117143).
- [76] Oral, C. B.; Su, E.; Okay, O. Silk Fibroin-Based Multiple-Shape-Memory Organohydrogels. *ACS Appl. Mater. Interfaces.* **2024**, 16, 56146–56158. DOI: [10.1021/acsami.4c12648](https://doi.org/10.1021/acsami.4c12648).
- [77] Yetiskin, B.; Okay, O. Berkant High-Strength and Self-Recoverable Silk Fibroin Cryogels with Anisotropic Swelling and Mechanical Properties. *Int. J. Biol. Macromol.* **2019**, 122, 1279–1289. DOI: [10.1016/j.ijbiomac.2018.09.087](https://doi.org/10.1016/j.ijbiomac.2018.09.087).
- [78] Hu, Y.; Suo, Z. Viscoelasticity and Poroelasticity in Elastomeric Gels. *Acta Mech. Solida Sin.* **2012**, 25, 441–458. DOI: [10.1016/S0894-9166\(12\)60039-1](https://doi.org/10.1016/S0894-9166(12)60039-1).
- [79] Noselli, G.; Lucantonio, A.; McMeeking, R. M.; DeSimone, A. Poroelastic Toughening in Polymer Gels: A Theoretical and Numerical Study. *J. Mech. Phys. Solids* **2016**, 94, 33–46. DOI: [10.1016/j.jmps.2016.04.017](https://doi.org/10.1016/j.jmps.2016.04.017).
- [80] Oyen, M. L. Mechanical Characterisation of Hydrogel Materials. *Int. Mater. Rev.* **2014**, 59, 44–59. DOI: [10.1179/1743280413Y.0000000022](https://doi.org/10.1179/1743280413Y.0000000022).
- [81] Lu, X. L.; Mow, V. C. Biomechanics of Articular Cartilage and Determination of Material Properties. *Med. Sci. Sports Exerc.* **2008**, 40, 193–199. DOI: [10.1249/mss.0b013e31815cb1fc](https://doi.org/10.1249/mss.0b013e31815cb1fc).
- [82] Mow, V. C.; Kuei, S. C.; Lai, W. M.; Armstrong, C. G. Biphasic Creep and Stress Relaxation of Articular Cartilage in Compression: Theory and Experiments. *J. Biomech. Eng.* **1980**, 102, 73–84. DOI: [10.1115/1.3138202](https://doi.org/10.1115/1.3138202).
- [83] Soltz, M. A.; Ateshian, G. A. Experimental Verification and Theoretical Prediction of Cartilage Interstitial Fluid Pressurization at an Impermeable Contact Interface in Confined Compression. *J. Biomech.* **1998**, 31, 927–934. DOI: [10.1016/s0021-9290\(98\)00105-5](https://doi.org/10.1016/s0021-9290(98)00105-5).
- [84] Malandrino, A.; Moendarbary, E. Poroelasticity of Living Tissues. In *Encyclopedia of Biomedical Engineering*; Hellmich, C.; Mantovani, D.; Wong, A.; Rymer, W. C.; Hargrove, L., Eds.; Elsevier: Amsterdam, 2019; Vol. 2, pp 238–245.
- [85] Suner, S. S.; Demirci, S.; Yetiskin, B.; Fakhrullin, R.; Naumenko, E.; Okay, O.; Ayyala, R. S.; Sahiner, N. Cryogel Composites Based on Hyaluronic Acid and Halloysite Nanotubes as Scaffold for Tissue Engineering. *Int. J. Biol. Macromol.* **2019**, 130, 627–635. DOI: [10.1016/j.ijbiomac.2019.03.025](https://doi.org/10.1016/j.ijbiomac.2019.03.025).
- [86] Sahiner, N.; Sengel, S. B. Various Amine Functionalized Halloysite Nanotube as Efficient Metal Free Catalysts for H₂ Generation from Sodium Borohydride Methanolysis. *Appl. Clay Sci.* **2017**, 146, 517–525. DOI: [10.1016/j.clay.2017.07.008](https://doi.org/10.1016/j.clay.2017.07.008).
- [87] Pavličáková, V.; Fohlerová, Z.; Pavličák, D.; Khunová, V.; Vojtová, L. Effect of Halloysite Nanotube Structure on Physical, Chemical, Structural and Biological Properties of Elastic Polycaprolactone/Gelatin Nanofibers for Wound Healing Applications. *Mater. Sci. Eng. C Mater. Biol. Appl.* **2018**, 91, 94–102. DOI: [10.1016/j.msec.2018.05.033](https://doi.org/10.1016/j.msec.2018.05.033).
- [88] Kurczewska, J.; Ceglowski, M.; Messyasz, B.; Schroeder, G. Dendrimer-Functionalized Halloysite Nanotubes for Effective Drug Delivery. *Appl. Clay Sci.* **2018**, 153, 134–143. DOI: [10.1016/j.clay.2017.12.019](https://doi.org/10.1016/j.clay.2017.12.019).
- [89] Liu, M.; He, R.; Yang, J.; Long, Z.; Huang, B.; Liu, Y.; Zhou, C. Polysaccharide-Halloysite Nanotube Composites for Biomedical Applications: A Review. *Clay Miner.* **2016**, 51, 457–467. DOI: [10.1180/claymin.2016.051.3.02](https://doi.org/10.1180/claymin.2016.051.3.02).